ISTANBUL TECHNICAL UNIVERSITY★GRADUATE SCHOOL OF SCIENCE ENGINEERING AND TECHNOLOGY

DIAGENESIS OF EOCENE AND OLIGOCENE SANDSTONES AND SHALES OF THE GAZİKÖY AND KEŞAN FORMATIONS IN THE THRACE BASIN

M.Sc. THESIS

Havva GURZALIYEVA

(50131305)

Department of Geological Engineering

Geological Engineering Programme

Thesis Advisor: Prof.Dr. Ömer Işık ECE

JUNE 2016

İSTANBUL TEKNİK ÜNİVERSİTESİ ★ FEN BİLİMLERİ ENSTİTÜSÜ

TRAKYA HAVZASINDAKİ EOSEN VE OLİGOSEN YAŞLI GAZİKÖY VE KEŞAN FORMASYONLARINDAKİ KUMTAŞLARI VE ŞEYLLERİN DİYAJENEZİ

YÜKSEK LİSANS TEZİ

Havva GURZALIYEVA

(50131305)

Jeoloji Mühendisliği Anabilim Dalı

Jeoloji Mühendisliği Programı

Tez Danışmanı: Prof. Dr. Ömer Işık ECE

Haziran 2016

Havva Gurzaliyeva, a **M.Sc.** student of ITU **Graduate School of Geological Engineering** with student ID of **505131305**, successfully defended the **thesis** entitled **"EOCENE AND OLIGOCENE SANDSTONE AND SHALE DIAGENESIS OF THE GAZİKÖY AND KEŞAN FORMATIONS, WESTERN MARMARA REGION, TEKİRDAĞ BASIN"**, which she prepared after fulfilling the requirements specified in the associated legislations, before the jury whose signatures are below.

Thesis Advisor: **Prof. Dr. Işık Ömer ECE** ....
Istanbul Technical University

Jury Members: **Assoc. Prof. Dr. Emin ÇİFTÇİ** ....
Istanbul Technical University

Prof. Dr. Hayrettin KORAL ....
Istanbul University

Date of Submission : 02 May 2016
Date of Defense : 10 June 2016

To my family,

FOREWORD

I wish to express thanks to all those who have helped and supported me in the completion of this Master thesis. I would like to thank my supervisor Prof. Dr. Ömer Işık Ece and Assoc. Prof. Dr. Emin Çiftçi, for their valuable and constructive suggestions during planning and progress of this work, and guidance during my stay at Istanbul Technical University (ITU).

My great appreciations go to Dr. Orhan Yavuz for his invaluable support, advice and encouragement throughout all the phases of the thesis project progress. I wish also to acknowledge the great support and assistance provided by Ismat Valiyev.

I would also like express great thanks to BP Caspian Exploration, Nippon Foundation for funding my MSc studies at ITU.

I am also thankful to my family, especially my mother, sister and close friends for their persistent and priceless encouragement and support throughout my MSc studies.

I would like to dedicate this study to my family: to my mother and sister.

June 2016

Havva Gurzaliyeva
Geological Engineer

TABLE OF CONTENTS

Page

FOREWORD..**ix**
TABLE OF CONTENTS...**xi**
ABBREVIATIONS…..**xiii**
LIST OF FIGURES……...**xv**
SUMMARY...**xvii**
ÖZET..**xix**
1. INTODUCTION **1**
1.1 Genral..1
1.2 Methodology...2
1.2.1 Sampling 2
1.2.2 Research methods 2
2. STUDY AREA **3**
2.1 Geographic and Geologic Overview 3
2.2 Facies 4
2.2.1 Scheme of classification 5
2.3 Stratıgrpahy...7
2.3.1 Gaziköy Formation..8
2.3.2 Keşan Formation...11
3. PETROGRAPHY AND DIAGENESIS OF THE SANDSTONES AND SHALES IN THE THRACE BASIN (Gaziköy and Kumbağ) **13**
3.1 Methods..14
3.1.1 Optical microscopy 14
3.1.2 X-Ray Diffraction (XRD)..14
3.2 Petrogrpaphy...14
3.2.1 Texture..15
3.2.2 Detrital mineral composition 21
3.3 Diagenesis and turbidite system...23
3.3.1 Cement and authigenic minerals 26
4. THE DIAGENESIS AND ASSOCIATION OF FACIES...**41**
4.1 DIAGENETIC RELATIONS.......…...41
4.1.1 D Facies (Pelitic-Arenaceous Facies 1) 41
4.1.2 E Facies (Pelitic-Arenaceous Facies 2) 42
4.1.3 E Facies (Chaotic Facies) 42
5. CONCLUSION **43**

REFERENCES..47
APPENDICES...51
APPENDIX A..51
APPENDIX B..52
APPENDIX C..53
CURRICULUM VITAE (CV)...55

ABBREVIATIONS

C	: Carbonate
Cal	: Calcite
Chl	: Chlorite
cm	: centimeter
Eoc	: Eocene
F	: K-Feldspar
Feld	: Feldspar
M	: Muscovite
m	: Microcline
mQ	: Monocrystalline quartz
Olg	: Oligocene
Plg	: Plagioclase
pQ	: Polycrystalline quartz
Q	: Quartz
R-F	: Rock Fragment
S	: Sample
μ	: micron

LIST OF FIGURES

Page

Figure 2.1 Google map of the study area which located in a Tekirdağ Province, Turkey. Our study area started from Gaziköy to Kumbağ regions. The samples are collected along this route..**4**
Figure 2.2 Geological map of Ganos Mountain and the surrounding region. For location see Fig. 2 (compiled from Lebküchner, 1974; Şentürk et al.,1998; A. Okay unpublished data) **8**
Figure 2.2.1 Generalized lithostratigraphic section of the Tertiary sediments of the Thrace basin (Siyako, 2006) **9**
Figure 2.3 The geology map of the Thrace Basin (Siyako and Huvaz, 2007) **10**
Figure 2.3.1 Simplified stratigraphic section through the Gaziköy and Keşan Formations along the north of the Ganos Faultn (Yatirak, 1995) **11**
Figure 2.3.2 A view from the Gaziköy Formation near Uçmakdere along the northern coast of the Marmara Sea **12**
Figure 3.2.1 Sample 59, photomicrograph, cross polarized light, plane polarized light...**16**
Figure 3.2.2 Sample 27, photomicrograph, cross polarized light, plane polarized light...**17**
Figure 3.2.3 Sample 4, photomicrograph, cross polarized light, plane polarized light...**17**
Figure 3.2.4 Sample 37, photomicrograph, cross polarized light, plane polarized light...**18**
Figure 3.2.5 Sample 50, photomicrograph, cross polarized light, plane polarized light...**18**
Figure 3.2.6 Sample 66, photomicrograph, cross polarized light, plane polarized light...**19**
Figure 3.2.7 Sample 43, photomicrograph, cross polarized light, plane polarized light...**20**
Figure 3.2.8 Sample 33, photomicrograph, cross polarized light, plane polarized light...**20**
Figure 3.2.9 Sample 46, photomicrograph, cross polarized light, plane polarized light...**21**
Figure 3.3 Stratigraphic relations of the Eocene formations in the Gelibolu Peninsula. Southern Thrace and Northern Thrace (Siyako, 2006) **24**
Figure 3.3.1 The figure depicts major elements of a turbidite system in a three-dimensional depositional model (redrawn from Mutti and Normak, 1991) **25**
Figure 3.3.1.1 Sample 4 – Eocene aged Sandstone..**30**
Figure 3.3.1.2 Sample 27 – Eocene aged Sandstone..**31**
Figure 3.3.1.3 Sample 33 – Eocene aged Shale...**32**
Figure 3.3.1.4 Sample 37 – Eocene aged Sandstone..**33**

Figure 3.3.1.5 Sample 43 – Eocene aged Shale..**34**
Figure 3.3.1.6 Sample 46 – Eocene aged - Oligocene Aged Shale (transitional sample) **35**
Figure 3.3.1.7 Sample 50 – Oligocene aged Shale..**36**
Figure 3.3.1.8 Sample 55 – Oligocene aged Sandstone...**37**
Figure 3.3.1.9 Sample 59 – Oligocene aged Sandstone...**38**
Figure 3.3.1.10 Sample 66 – Oligocene aged Shale...**39**

DIAGENESIS OF EOCENE AND OLIGOCENE SANDSTONES AND SHALES OF THE GAZİKÖY AND KEŞAN FORMATIONS IN THE THRACE BASIN

SUMMARY

The sandstone and shale samples from the Keşan and Gaziköy Formations in the Kumbağ, Tekirdağ, West of Istanbul have features of different facies of turbidities. For the basin analysis, we need interpretation of the sedimentary rocks of their depositional environment. The diagenetic evolution of these sandstones and shales caused many changes in porosity and permeability developments and their grain morphologies. Hence the composition and structure of the grain surface have to be known and their influences on pore walls and connection paths. The major issue of this study is to determine on the pore geometry and the grain surface roughness, which were formed from the authigenic minerals during diagenetic changes. Samples are analyzed by using some technical analysis such as X-ray Diffraction (XRD) for investigation crystal habits of authigenic minerals and cement textures. Rock composition is revealed by optical microscopy.

It is observed that the constituent of the sandstone and shale is mainly quartz, feldspar, plagioclase and small amounts of igneous rock fragments, deposited in deep sea environments. The detrital grains experienced variations in grain morphology, the shape of the pore space formed between grains depended on diagenetic conditions. Most of the grain surfaces are coated with chlorite, and chlorite authigenic minerals and some of them are covered with authigenic quartz and/or alkali feldspars. Pore spaces are found to be largely filled by calcite and subordinate anhydrite. The authigenic minerals: quartz, alkali feldspar, muscovite and chlorite also appear as pore – fillings. Authigenic minerals often overlap the grain surface leading to roughened pore walls, narrowed pore throats and deformed pore geometry.

The analysis of the grain morphology of five sandstones and 4 shales which were taken from Gaziköy and Keşan formations reveals that authigenic and cement minerals entirely covered the surface of grains. The other authigenic minerals: quartz, alkali feldspars, muscovite, chlorite and calcite cover some of the grain surfaces so that their roughness values only represent a partial roughness value.

All results obtained in this work reveal the influence of the grain roughness on the pore shape, the permeability of the rocks and on the wetting and the adhesion properties of the grain surface. The results of this study will allow to interpret diagenetic facies differences in various turbidite facies.

In this work, the mineral composition of sedimentary rocks (sandstone and shale) and the source of clastic grains, their textures and depositional setting are shown. The post depositional alterations and their influences on the grain morphology and pore geometry of sandstone and shale rocks from the Keşan and Gaziköy Formations in the Kumbağ, Tekirdağ, Western Marmara are studied. The authigenic mineral growth into the pore spaces and on the grain surfaces is investigated. The fine structure and the roughness of the authigenic minerals are determined. The characteristics of sandstone rocks, the diagenetic history, their pore geometry and grain surface features are

revealed. The results show that properties of the grain surface are complicated due to varying authigenic minerals covering the grains.

The methods used and the results obtained in this thesis contribute to a better determination of the grain surface characteristics and understanding of facies differences of turbidites. Therefore, the main achievements of this thesis are the identification of transition region of facies and various characteristics of different types of turbidite facies.

TRAKYA HAVZASINDAKİ EOSEN VE OLİGOSEN YAŞLI GAZİKÖY VE KEŞAN FORMASYONLARINDAKİ KUMTAŞLARI VE ŞEYLLERİN DİYAJENEZİ

ÖZET

Batı İstanbul, Tekirdağ, Kumbağdaki Gaziköy ve Keşan Formasyonlarindan alınan kumtaşı ve şeyl kayaçlarından alınan örnekler, farklı özellikli turbidite fasiyesleri var. Havza analizi için çevrede depolanmış sedimentar kayaçların yorumlanmasına gerek duyuyoruz. Bu kumtaşı ve şeyllerin diajenetik evrimi gozeneklik ve geçirgenliğin gelişiminde çoklu sayda değişikliklere neden oluyor. Tane yüzeyinin bileşiminin, yapısının ve onlarin gözenek duvarları ve baglantı yollarının bilinmesi gerekiyor. Bu çalışmanın esas amacı diajenez zamanı oluşan gözenekleri, tane yuzeyinin pürüzlülüğü, geçirgenlik ve fasiyesleri belirlemek. Örneklerin, otijenik mineralların ve çimento dokusunu araştırmak için X- ray Diffraksyon (XRD) gibi teknik analiz yöntemi kullanıldı. Kayaç bileşimi optik mikroskopla ortaya çıkarıldı.

Kumtaşı ve şeylin içeriğinin çoğunlukla nehir ve derin deniz ortamlarinda depolanan kuvars, feldspar, plajiyoklaz ve küçük volkanik kayaç fragmanlarindan olması gözlemlendi. Diajenetik durumlardan asılı olarak döküntülü tanelerde tanecikler farklılık gösteriyor. Tane yüzeylerinin bir çoğu klorit ve otijenik mineral kaplamalı, ve bazıları otijenik kuvars ve alkali feldspar kaplamalıdır. Gözenek alanları genellikle kalsit ve ikincil anhidritlerle doludur. Kuvars, alkali feldspar, muskovit ve klorit gibi otijenik mineraller gözenek alanlarinda dolgu malzemesi görevi taşıyor.

Gaziköy ve Keşan Formasyonlarından aldığımız örneklerin (5 kumtaşı ve 4 şeyl) tane morfoloji analizine göre otijenik ve çimento mineralleri tane yüzeyini tamamen kaplıyor. Kuvars, alkali feldspar, muskovit, klorit ve kalsit gibi otijenik mineraller tane yüzeyini kaplayarak kısmi pürüzlülük değerini belirliyor.

Elde ettiğimiz bütün sonuçlara dayanarak tane pürüzlülüğünün boşluk şekline, kayaçın geçirimliliğine ve tane yüzeyinin yapıştırma özelliğine etkisini söyleye biliriz. Bu çalışmanın sonucu bize turbiditlerde bulunan farklı çeşit diajenetik fasiyesleri yorumlamamızda yardımcı olabilecektir.

Bu çalışmada, sedimanter kayaçrın (kumtaşı ve şeyl) mineral bileşimi, kırıntılı kayaçların kaynağı , bunların doku ve depolanma oluşumu gösterilmiştir. Batı Marmara Tekirdağ arazısinde Keşan ve Gaziköy formasiyonlarında oluşan çökelme sonrası değişiklikler ve onların kumtaşı ve şeyl kayalarının tane morfolojisi ve por geometrisi üzerindeki etkileri incelenmiştir. Otijen minerallerin tane yüzeyinde olan büyüme prosesi incelenmişti. Otijen minerallerin ince yapısı ve pürüzlülüğü belirlenmişdi. Kumtaşı kayalarının özellikleri, onların por geometrisi ve tane yüzey özellikleri ve diyajenetik tarihi ortaya çıkarılmıştı. Sonuçlar değişen otijenik

minerallerin taneleri kaplama nedeniyle tane yüzeyinin karmaşık özelliklerinin olduğunu göstermektedir.

Kullanılan yöntemler ve bu tezde elde edilen sonuçlar tane yüzey özelliklerinin belirlenmesinde ve türbiditlerin fasiyes farklılıklarının anlaşılmasında daha iyi bir katkıda bulunur. Bu nedenle, bu tezin temel başarılarından biri fasiyes geçiş bölgesinin ve farklı tür türbidit fasiyeslerin çeşitli özelliklerinin belirlenmesidir.

1. INTRODUCTION

1.1 General

Every type of basin analysis increasingly requires an interpretation of sedimentary rocks in terms of their depositional environment. The particular task of sedimentology is the development of practical criteria useful to the geologist in the field for distinguishing facies and associations of facies that are significant objectives of basin analysis.

The most logical approach to the determination of such criteria has always been the comparison of features of recent sediments, whose depositional environments are known, with ancient sediments, whose environments we wish to determine. Substantial progress has been made on this basis in the understanding of major depositional environments of clastic rocks and (more recently) carbonate rocks deposited in continental or shallow-marine environments. Turbidities, which are sediments of pre-eminent importance for the analysis of many basins, have particularly suffered in this manner from limitations in employment of actualistic criteria. They seem at present to form an artificial category of deposits that are bound more to hydrodynamic models of transport and distribution than to environmental description that are geologically significant.

In this work recent analytical developments applied in scientific fields such as in geosciences, are thus used to characterize the morphology of mineral grain surfaces and to investigate facies of turbidites by using sandstone and shale rocks. Moreover, the fine surface structures and roughness of the authigenic minerals, which are formed during diagenesis, are studied. The grain surface roughness is one of the factors that significantly impact on difference properties of facies and permeability of sandstone and shale rocks.

The study in this thesis discusses the characteristics of sedimentary grains of sandstone and shale rocks. The grain features are altered due to diagenesis and show thus variations in grain morphology, surface roughness and pore geometry.

The findings of this thesis reveal the diagenetic history of sandstone and shale rocks, grain morphology, grain surface roughness and a detailed insight into the geometry of pore spaces.

1.2 Methodology

1.2.1 Sampling

To study petrography, diagenesis of sedimentary rocks, characteristics of sedimentary grains and pore space geometry in sandstone and shale rocks, sandstone samples were collected from the Keşan and Gaziköy Formations in the Kumbağ, Tekirdağ, Western Marmara. Then, selected samples were analyzed by thin section petrography, pore geometry, grain morphology and grain roughness. The analytic methods used were Optical Microscopy, X–ray Diffraction (XRD). Also, software XRD Commander were applied to analyze data.

Petrographic and diagenetic studies are available for 36 set of samples. Ten of sample sets marked (S4, S27, S33, S37, S43, S46, S50, S55, S59 and S60) (see appendix I.1) were selected to investigate grain morphology, pore geometry, surface roughness. Selection of these samples was based on their mineralogy, porosity and sedimentary texture.

1.3.2 Research methods

The different analytical steps of each method applied in this study are described in detail in the general introductions to the different chapters.

Petrographic analysis with optical microscope was used to determine grain shape, grain size and mineral composition of rock. Distributions of detrital grains, cement of rock and estimation of pore space between grains are revealed. The coatings surrounding grains by authigenic minerals or sharp crystal structure of authigenic quartz could be observed in thin section. Crystal habits of authigenic minerals and cement textures were determined and combined chemical element analysis by X-ray Diffraction (XRD).

Subsequently, the samples marked S4, S27, S33, S37, S43, S46, S50, S55, S59 and S60 were investigated for pore geometry, grain morphology and surface roughness analyses.

Optical Microscopy were used for enhancing the composition of rocks, analyzing pore space morphology and grain geometry. The determination of the rock components was done via the Optical Microscopy at each imaged point on grain surface.

2. STUDY AREA

2.1 Geographic and Geologic Overview

The geological structure of Tekirdağ is quite young. At the I. Period the city was covered with the sea. Meanwhile the terrestrial based sediments came into existence at the bottom of the seas because of the erosions. At the II. Period, with the effects of the Alps folds, both the North Anatolian and Tekir Mountains came into being. The old sedimentary and basic layers were broken and curled. At the end of the III. Period, in the Neogene, the Tekir Mountain was opened again and became straight. At this period, marns were massed in the plateau that is on the north side of Ganos and Koru Mountains.

1. Formation of Keşan – It is formed with sandstone, pebblestone in the shape of lens and other volcanic rocks.
2. Formation of Gaziköy – It is formed with coarse-grained sandstones and things with tuff.

Although primarily a transform fault, along its entire length the North Anatolian Fault (NAF) zone is associated with uplifts and depressions related to segmentation and bending. The most prominent active depressions are the three basins, over 1000 m deep, which are forming along its main strand in the Sea of Marmara (Wong et al., 1995; Okay et al., 2000; LePichon et al., 2001; Armijo et al., 2002).

Ganos Mountain forms essentially a single range made up of similar lithology, is relatively small, and has uniform orientation. These geomorphic features, coupled with the high rate of deformation in the region, indicate that the morphology of the mountain can be used to chart recent vertical crustal motions.

Our study area started from Gaziköy to Kumbağ regions. The samples are collected along this route.

2.2 Facies

Despite the apparently monotonous character of turbidite successions that constitute the various flysch units of the Northren Appenines, rather well-defined facies and associations of facies indicative of different depositional processes and environments

Figure 2.1 : Google map of the study area which located in a Tekirdağ Province, Turkey.

Mutti and de Rosa (1968), and Ricci Lucchi (1969); herein we discuss and propose the most successfully adopted criteria and terminology for the study. First, however, it is appropriate to clarify our use of the terms facies and associations of facies.

Facies or lithofacies are used herein to indicate a group of strata, or less commonly a single stratum, with well-defined lithology, stratification, sedimentary structures and association of facies is the combination of two or more facies in a broader spatial arrangement.

The characteristics of facies reflect as a rule only the mechanism of deposition. The characteristics of an association of facies express the variations in time and space of the above-mentioned process and therefore furnish the most important elements for environmental interpretations.

2.2.1 Scheme of classification

Schematically, the more common turbidite facies are limited to following types:

A. Arenaceous-Conglomerate Facies
B. Arenaceous Facies
C. Arenaceous-Pelitic Facies
D. Pelitic-Arenaceous 1
E. Pelitic-Arenaceous 2

Intercalated in the above facies are other facies that are not strictly turbiditic, such as those related to submarine land sliding and ultimately to the other types of the formation such as current drag (Ricci Lucchi, 1969b) and those related to so-called “normal” sedimentary mechanisms. This facies which we will call “associated” in a general sense, are the following:

F. Chaotic Facies
G. Hemipelagic and Pelagic Facies

All of the above facies can be grouped into the following facies associations:

1. Slope of scarp associations
2. Deep-sea fan or proximal basin associations
3. Deep-sea plain or distal basin associations

Based on our analysis for our region we have D, E and F facies.

D. Pelitic Arenacous Facies 1:

The most important characteristic of this facies is that the beds are absolutely plane-parallel and persist laterally for hundreds or thousands of meters (in certain cases, tens of kilometers). Each one of these beds consists of lithologic couplet as in facies C, but the pelitic part is generally of greater thickness and the arenaceous part is finer grained (fine or very fine-grained sand and coarse – grained silt). The arenaceous part is entirely laminated with thin laminae most common. The sand/ shale ratio ranges in general from 1:2 to 1:9 and the thickness of the arenaceous part in general from 3 to

40 cm; the arenaceous part in some cases may disappear almost completely or, in contrast, may be more than one meter thick. In terms of Bouma sequence, these beds lack one or more of the basal units Tb-e, Tc-e, Td-e, and T-e. The Tc-e type is the modal sequence and the most commonly present.

Rigid application of Bouma's model as with Facies C, causes some difficulties in this facies with regard to the reciprocal relations of various types of current laminae, both in horizontal and vertical senses; the relations are in many ways more complex than the model predicts. Sole markings are less developed than in Facies C, especially in their dimensions, a tool marks tend to be most common. In contrast with Facies C, markings between laminae are very abundant and general found between laminae that are richer in politic matrix, mica and small plant fragments. The turbidite deposits of these facies may be represented at one extreme by only the Te sequence or entirely politic turbities; this can be recognized as such by the contrast in lithology and faunal content with respect to the associated hemipelagic sediments.

E. Pelitic-Arenacous Facies 2

This facies is included the same general grouping as the preceding one, namely the category of "distal" turbidites of Walker (1967), mainly because of the reduced thickness of the sandstone part. Nevertheless, we believe that this facies has major characteristics that differ from those of facies D. This will be stressed in the paragraphs related to the environmental interpretation of the facies, and include:

1. Smaller thickness of the individual strata, which are generally less 30 cm and more frequently less than 15 cm thick;
2. A higher sand: shale ratio, commonly about or greater than 1:1;
3. A coarser grain size and lower sorting index;
4. A marked irregularity of the surfaces of stratification: pinch-and-swell, flaser and lenticular bedding;
5. The presence of basal graded and structureless intervals;
6. The presence intraformational inclusions; and
7. A distinct separation, commonly visible between the aeranecous and pelitic parts.

F. Chaotic Facies

Within this vast category we grouped for convenience all deposits that originated within rather than outside the sedimentary as a result of remobilization by either massive sliding or tangential slips, independent of the ultimate or immediate cause of the collapse and of the rheological behavior of the materials. Many aspects of this deposits can be studied such as their composition, the intensity and style of deformation, and then scale of deformation. The term chaotic is used here in a general sense, and includes mild and /or localized deformation of beds. Excluded, however, are chaotic intervals or levels within individual beds, which belong to other facies.

2.3 Stratigraphy

Stratigraphically, Ganos Mountain forms an uplifted part of the hydrocarbon-bearing Mid-Eocene to Oligocene sequence of the Thrace Basin (Kopp et al., 1969; Turgut et al., 1991; Görür and Okay, 1996). This consists mainly of siliciclastic turbidites and is more than 9 km thick in its central part. These sedimentary rocks are weakly deformed except along the active North Anatolian fault and the inactive Terzili fault of Miocene age. Ganos Mountain exposes these Eocene–Oligocene siliciclastic rocks, which are divided into four formations. The oldest, the Gaziköy Formation, consists mainly of Eocene shale and siltstone with rare sandstone and andesitic tuff and basaltic lava interbeds, and represents distal turbidites (Aksoy, 1987). Its base is not exposed, but it has a minimum measured thickness of 855 m and gradually passes up to the sandstone–shale intercalation of the Keshan Formation. The Keshan Formation has a thickness of over 3 km at Ganos Mountain and consists of Upper Eocene proximal turbidites. It is overlain conformably by shales of the Mezardere formation, 750 m thick, representing prodelta mudstones. These shales are overlain by the thickly bedded Oligocene sandstones of the Osmancık Formation.

The stratigraphy south of the Ganos Fault is different. In this region, which is morphologically not part of the Ganos Mountain, a sandy Miocene sequence, more than 1 km thick, unconformably overlies turbiditic Eocene–Oligocene siliciclastics exposed in the cores of faulted anticlines (Fig. 6; Okay et al., 1999; Sakınç¸ et al., 1999; Yaltırak and Alpar, 2002). This difference is caused by the vertical movements along the North Anatolian Fault, which led to the erosion of the Miocene sequence north of the fault, as well as by the right-lateral offset on the North Anatolian Fault,

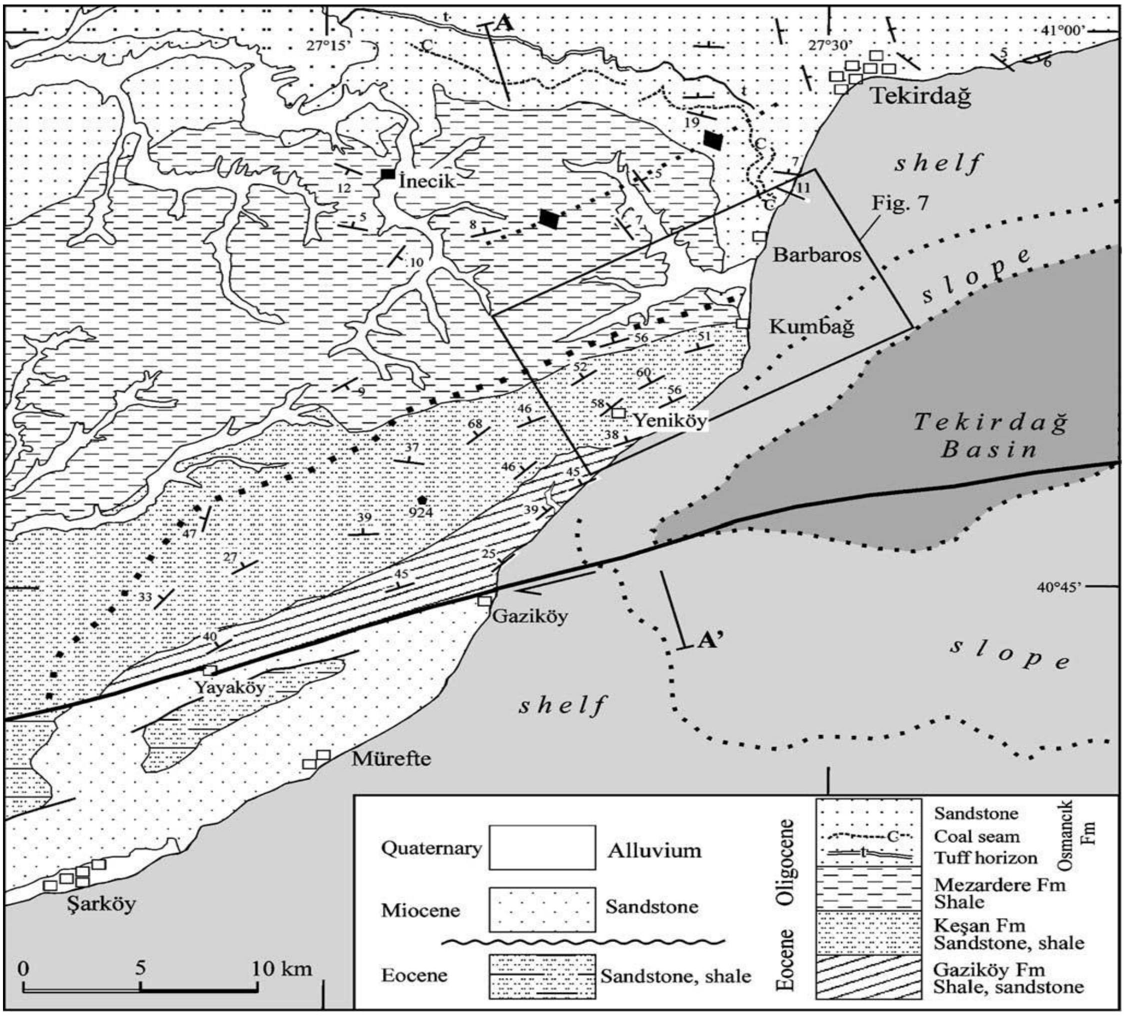

Figure 2.2: Geological map of Ganos Mountain and the surrounding region. For location see Fig. 2 (compiled from Lebküchner, 1974; Şentürk et al.,1998; A. Okay, unpublished data).

which now juxtaposes regions that were previously separated by distances of tens of kilometers.

2.3.1 Gaziköy formation

Gaziköy Formation was firstly identified by NV Turkse Shell (1972). Its outcrops extend along southern flanks of Ganosdağ in the northern shoreline of the Marmara Sea (Figure 2.3). Marmara Sea and the intense deformation of the Ganos Fault prevent to observe the base of the Gaziköy Formation. It underlies the Keşan Formation with

a gradual contact (Figure 2.3.2). Gaziköy Formation is composed of interbedded thin sandstone, siltstone and dark gray shale lithologies with tuff intercalations. As

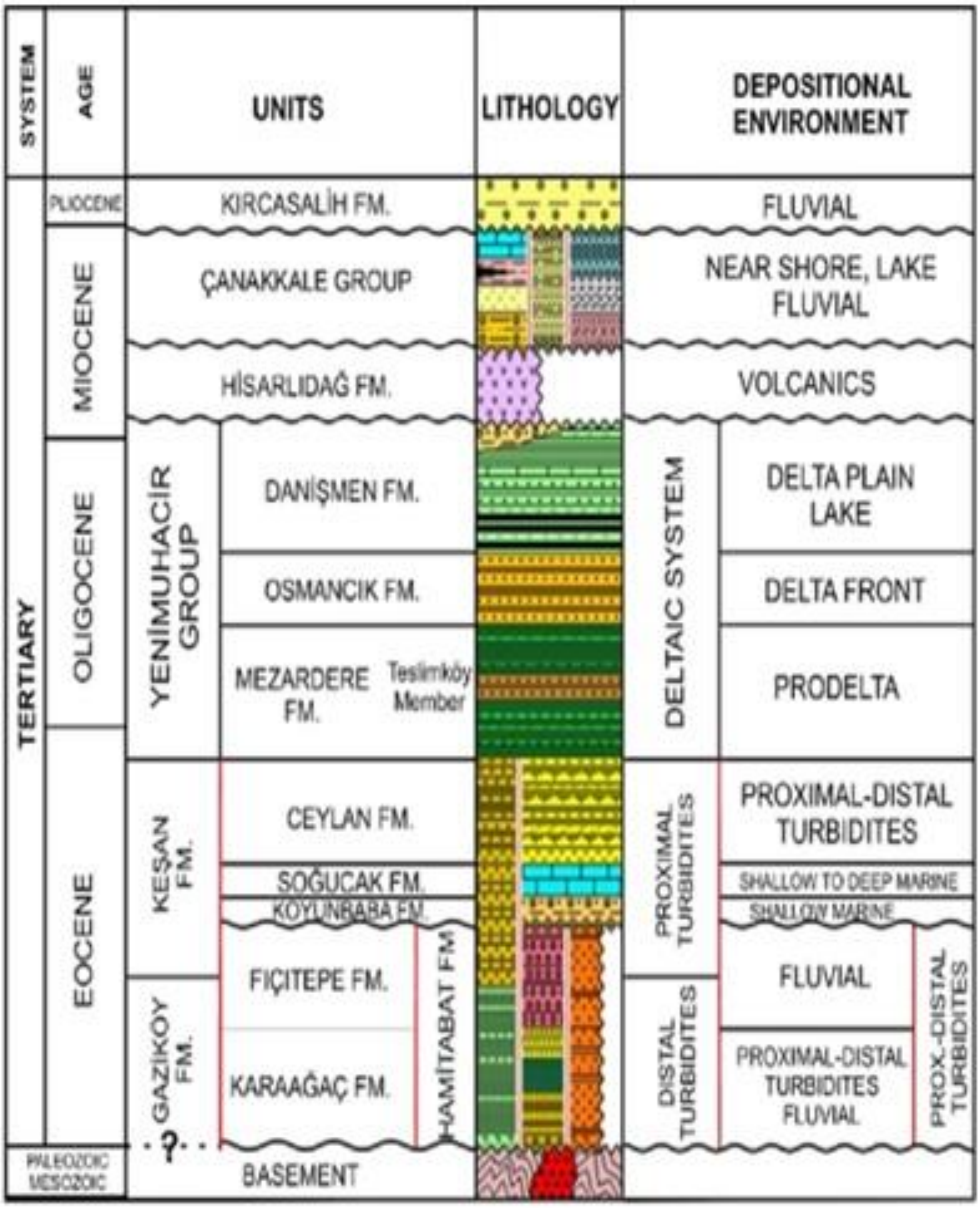

Figure 2.2.1: Generalized lithostratigraphic section of the Tertiary sediments of the Thrace basin (Siyako, 2006).

dominant lithology is shale, grain size and thickness of sandstone beds increase upward gradually (Yaltırak, 1995). They have sharp base and gradual top with siltstones. The various sandstone bed thicknesses from base to top, missing Ta and Tb divisions in Bouma (1962) sequence, the absence of basal sedimentary structures, the existence of thin laminated sandstone beds, the increase in mud-sand ratio downward, high organic content and non-variable bed thicknesses along high distances indicate that the Gaziköy Formation is deposited in a wide deep marine environment as middle

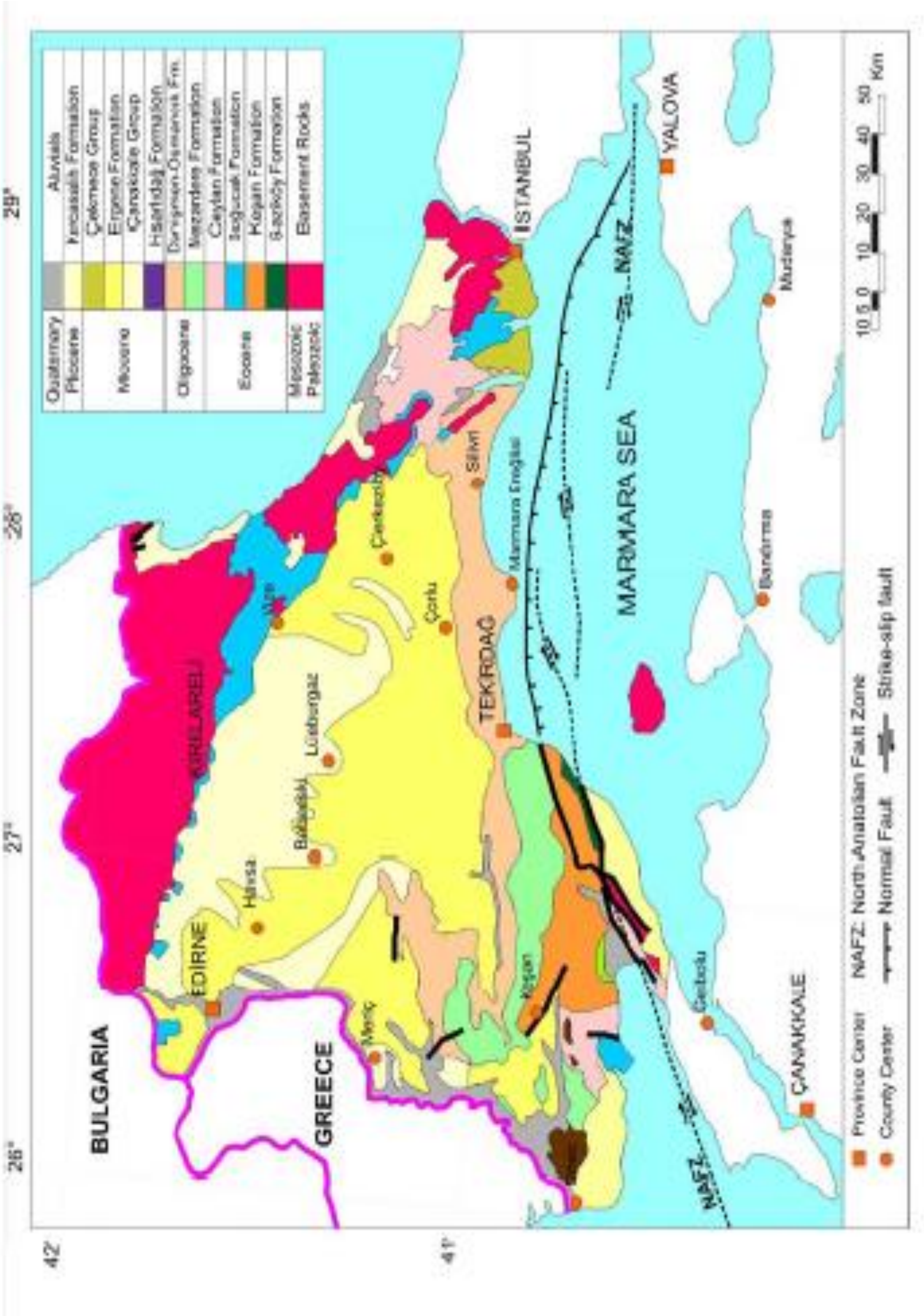

Figure 2.3: The geology map of the Thrace Basin. Most of the area is covered by the Miocene Ergene Formation (yellow color) and the Pliocene Kırcasalih Formation (pale yellow color). The map was taken form Siyako and Huvaz (2007)

to distal turbiditic facies (Yaltırak, 1995). Depositional model of the Gaziköy Formation may resemble the outer fan of the sub-marine fan model of Normark (1978) (Figure 2.3.2). Based on nannoplanktons, a Middle-Late Eocene age has been assigned to the Gaziköy Formation (Sümengen and Terlemez, 1991).

2.3.2 Keşan Formation

Keşan Formation was identified firstly by Gökçen (1967). Keşan Formation has gradual contacts with the underlying Gaziköy Formation and the overlying Mezardere Formation (Figure 2.3.2). The outcrops of the Keşan Formation extend from Kumbağ to the Saros Bay in the south of the Ganos Fault (Figure 2.3). According to Sümengen and Terlemez (1991) lithology description, the formation is composed of thinly bedded, fine-grained sequence of sandstone, siltstone, mudstone lithologies and sequences of medium to coarse-grained, moderately to thickly bedded fining upward channel fill sandstones which show lateral discontinuities. A view from the Keşan Formation at the northern flank of Işıklar (Ganos) Mountain. The characteristic features of a typical turbiditic sequence (Yaltırak, 1995) were observed. Each sequence initiates with massive to well-bedded pebbly sandstones with a largely

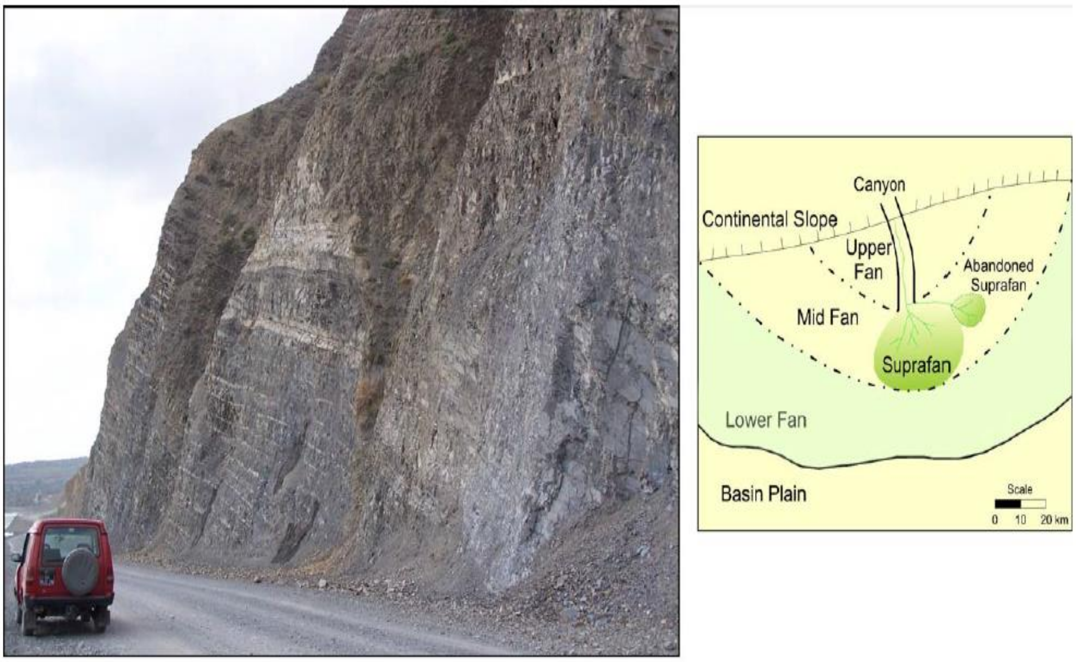

Figure 2.3.1: A view from the Gaziköy Formation near Uçmakdere along the northern coast of the Marmara Sea. The depositional environment of the Gaziköy Formation resembles the lower sub-marine fan model of Normak (1978).

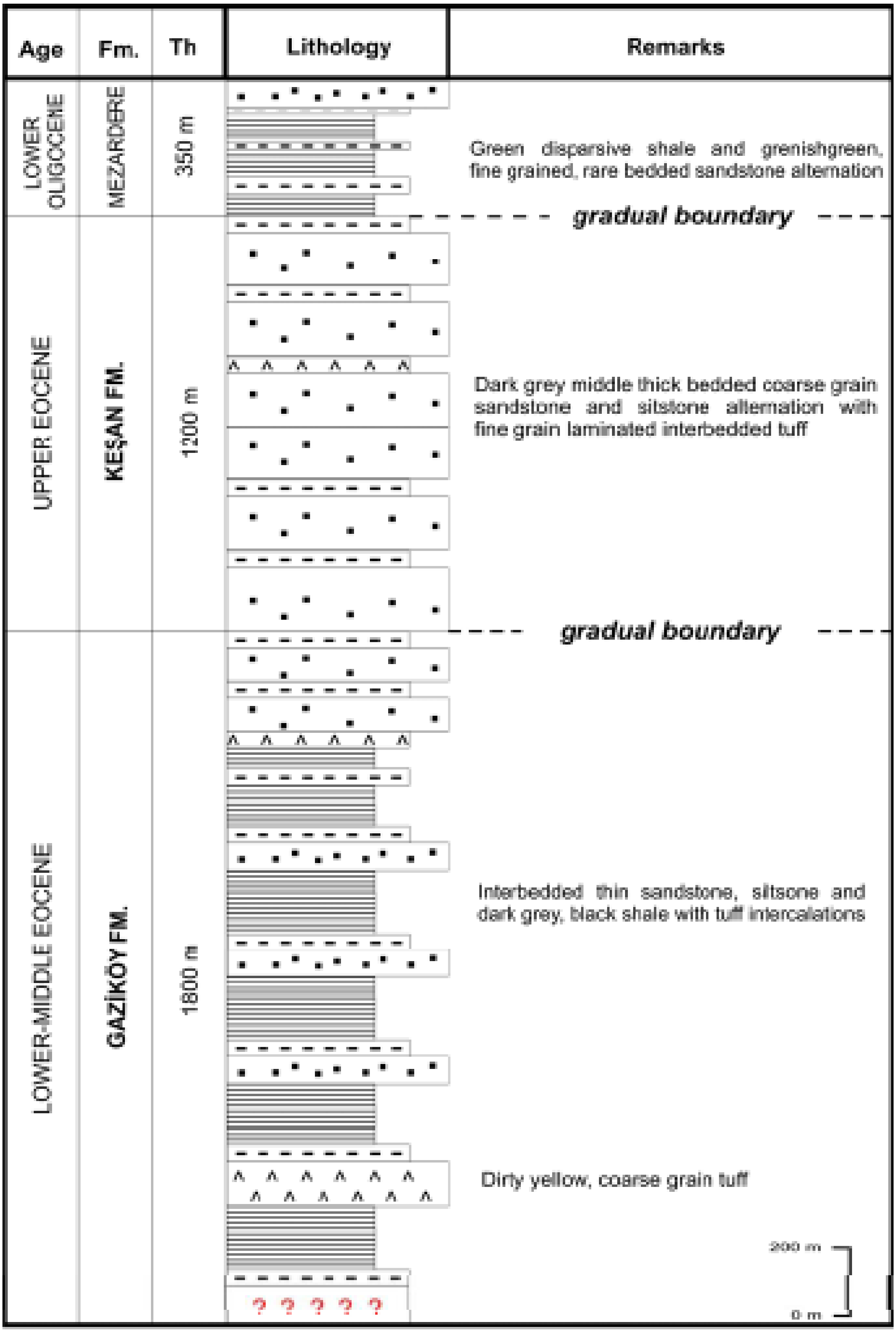

Figure 2.3.2: Simplified stratigraphic section through the Gaziköy and Keşan Formations along the north of the Ganos Fault (from Yaltırak, 1995).

eroded base. This pebbly bearing level grades upward into medium to coarse-grained, moderately to thickly bedded sandstone. Ta, Tb and Tc-divisions of Bouma (1962) sequence are well developed. These sequences are overlain by massive mudstones. The sandstone intervals of varying thicknesses are encompassed by another sandstone dominated sequence, consisting of fine-grained sandstone, siltstone and claystone. The most diagnostic features of sandstone beds within this interval are that they have sharp upper surfaces with current ripples and laterally thin out at a short distance and finally pass into mudstones. Siltstones and claystones are commonly massive and display parallel laminations on millimeter to centimeter scales locally. These characteristic features for the turbiditic section of the Keşan Formation resemble mid-fan of the submarine fan model of Normark (1978). In addition, volcanic matrix of sandstone beds indicates that volcanic activity was active during the deposition (Turgut et al., 1983). Based on nannoplanktons, the age of the Keşan Formation was given as Late Eocene by Sümengen and Terlemez (1991).

3. PETROGRAPHY AND DIAGENESIS OF THE SANDSTONES AND SHALES IN THE THRACE BASIN (GAZİKÖY AND KUMBAĞ)

The investigation of the petrography and diagenesis of sandstones and shales of the Tekirdağ Basin reveals the sediment provenance, depositional environments and history of post – depositional alterations. Sedimentary rock petrography in general, concentrates on the detail description of the composition and the textural relationship of the rocks. Clastic grains are packed together in fine grained matrix and cement. The constituents of the sandstone samples permit identification of the source of rocks. All the investigated sandstones are quartz-rich, also containing feldspar, locally abundant volcanic rock fragments, indicating that the clastic grains derived from weathered igneous and/or volcanic rocks. The sandstones with well-rounded to rounded clastic grains indicate the textural maturity related to sediment recycling of the deposits in bed load transport. The sediments with laminations are recognizable as an accommodation in multiple phases of fluvial or shallow water marine or lacustrine reworking. The precipitation of authigenic minerals and cements in pore spaces and surrounding grains during diagenesis is shown. Less stable minerals as feldspars and volcanic fragments are dissolved and replaced by authigenic minerals. The growth of diagenetically formed clay minerals narrows pore spaces and roughens pore walls and pore throats leading to reducing storage capacity, changes in fluid/rock wetting properties and in fluid flows through pores in the sandstones.

3.1 Methods

3.1.1 Optical microscopy

Thin sections were prepared of 5 sandstones and 5 shales samples from the observed region. Pores within the sandstones and shales were stained blue by epoxy resin. Thin sections were either polished or covered with glass after staining. All thin sections were studied with a Leica DM 2500M petrographic microscope under plane and cross polarized light. The investigation describes the characteristics of detrital, authigenic mineralogy, porosity, and texture. The samples showed some alternating lamination of coarser and finer grains and differing cement and pore space volume.

3.1.2 X-Ray Diffraction (XRD)

The samples marked S4, S27, S33, S37, S43, S46, S50, S55, S59 and S60 were separated into two groups, such as sandstones and shale and mounted on top of a conical sample holder. Crystal morphology of the authigenic minerals, type of authigenic minerals, their relationship to framework grains and pore network were examined and mineralogical analysis was done by X-Ray Diffraction (XRD). This analysis reveals the texture and fabric of sandstones and shales and aids to recognize the post depositional alteration. For this purpose, the samples were coated with a gold layer in an SCD 050 sputter coater. The sputter coater was operated for 40 seconds at a current of 40 Volts. The resulting gold film was only about 10 nm thick, to improve the resolution.

3.2 Petrography

Petrographic investigation is dealing with the source, occurrence, structure and history of rocks, especially sedimentary rocks. The classification or terminology of the sedimentary rocks was used in relevant fields as description of the composition, properties and classification of rocks by Folk (1974, 1980; Pettijohn, 1975). The source of sedimentary rocks was investigated by Pettijohn et al., (1972). This study refers to textural maturity, mineralogical classification, sediment provenance, which can be diagnostic an environment of deposition.

The sandstone and shale rocks studied from the Tekirdağ Basin, the Western Marmara Region, are fine to medium in grain size, moderately to well sorted and rounded to well-rounded in grain shape. The most abundant component of the sandstone and shale rocks is quartz with pale, milky, greyish brown colour, leached and weathered alkaline feldspar and plagioclase and rock fragments. Calcite dominated carbonate cement usually fills the pore spaces. The pore spaces are generated by arrangements of detrital grains and ranging from 5 % up to 20 %. The pores are occluded due to the precipitation of the authigenic minerals as quartz, albite, anhydrite, clays and calcite during diagenesis.

3.2.1Texture

The sediment distribution is not uniform, where sandstones are laminated by intercalation of very fine grained sediments (Appendix I.1_4146, Figure 3.2.1) and sometimes are interbedded by a thick layer of very fine sandstone, as seen at the depth of 2111 m and 4797 m (Appendix I.1_2111, Figure 3.2.2). These demonstrate that the sediments were deposited in a basin in which environmental conditions were unstable and flow velocity changed.

Most of the sandstones contain a little clay fraction. The sorting of grains is moderate to well. Diagrams are used to visually illustrate and estimate the sorting of sediments (Pettijohn, 1975) (see appendix I.2). However, in the laminated sandstones the sorting of the grains varies from laminae to laminae, but the sorting is not very high. The coarser sand grains always contain the finer grains embedded in between (Figure 3.2.1). The sand grains are rounded to very rounded (Figures 3.2.3 and 3.2.4), based on categories of roundness from low to high sphericity (Pettijohn, 1975), (see appendix I.3). However, rounding and sphericity of fine grains are less and less developed than in the medium and coarse grains (Figures 3.2.5, 3.2.6 and 3.2.7). The abundant grain size varies from 0.2 mm to 0.5 mm in diameter, although it is sometimes larger than 0.5 mm in diameter (Figure 3.2.4) or below 0.1 mm in diameter (arrows in figures 3.2.1 and 3.2.2), using the Udden – Wentworth scale: clay size is less than 0.039 mm; silt: 0.039 – 0.0625 mm; sand: 0.0625 – 2 mm etc. (see appendix I.3).

The grain distribution is of high density. The grain to grain contacts are mainly parallel to the long axis of the grains (Figure 3.2.8), suggesting that the grains were compacted mechanically. At higher depth the grains are more compacted, so many of the contacts between grains have undergone solution leading to the penetration of one grain into another. Therefore, the grain contacts are concavo – convex (Figures 3.2.9 and 3.2.10), and where solution is more intense, the contacts between grains become sutured (Figures 3.2.10 and 3.2.11).

The large rock fragment (R-F) in the middle of the photomicrographs is embedded in finer grains. Most of them are less than 0.25 mm in diameter. They are fine sand grains with subangular to subrounded grain shape and sometimes elongated. The sorting of grains is moderate to good. The sandstone is laminated, with laminae being defined by changes in grain size. The sorting of grains changes from laminae to laminae, but in

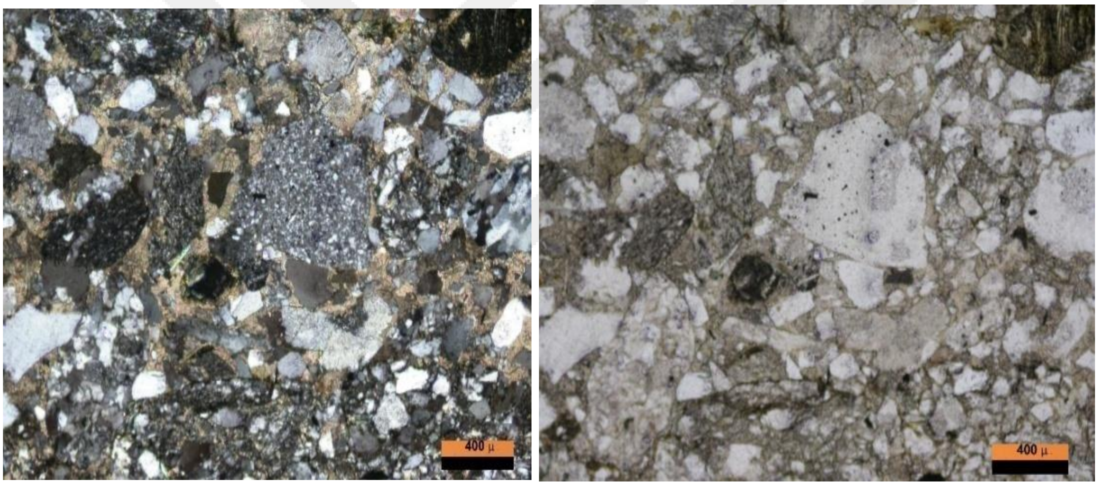

Figure 3.2.1: Sample 59, photomicrograph, cross polarized light, plane polarized light.

larger grain laminae, the coarser sand grains always contain the smaller grains between the large one. The coarse grains are ca. 0.3 mm in diameter and finer grains are less than 0.1 mm in diameter. Pore spaces have been filled by carbonate (C). There is the secondary growth of Quartz (Q). The ratio of minerals in this sample is 80 % Quartz (Q), 5-10 % Alkali Feldspar (Feld; Plg), 5-10 % Chlorite, 1% Muscovite, 1 % Opaque.

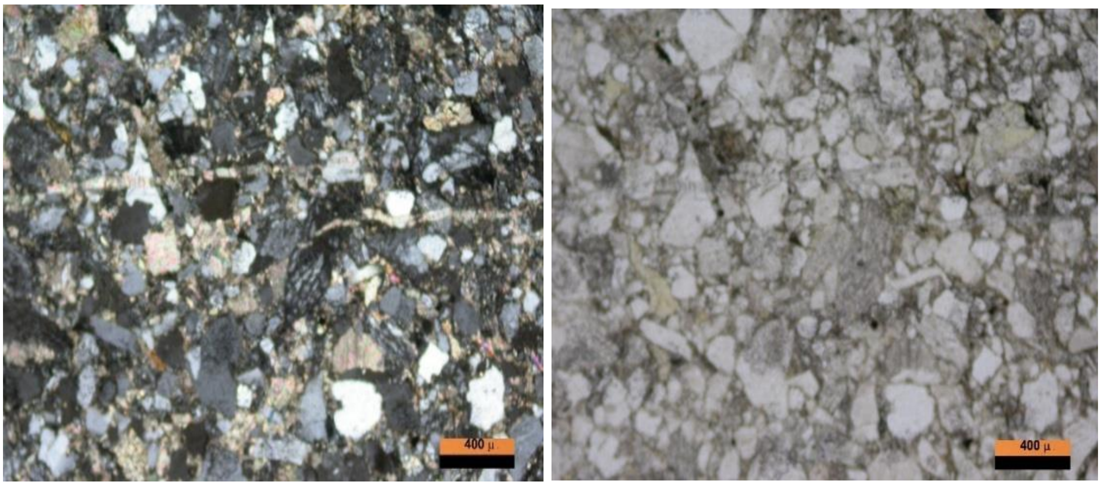

Figure 3.2.2: Sample 27, photomicrograph, cross polarized light, plane polarized light.

This coarse sandstone contains abundant quartz (Q), feldspar, plagioclase grains (Plg), muscovite (M) and rock fragments such as chert and recrystallized sparitic calcite (Cc) with grain sizes larger than 0.5 mm in diameter. The grains are poorly rounded. The sorting of the grains is moderated to bad. The grain contacts are concavo – convex and sutured (arrows). The sandstone is densely packed and compacted. Most of the pore spaces are filled by calcite cement (Cc). No open pores can be seen. The ratio of minerals is 40 % Quartz, 15-20 % Feldspar, 30 % Calcite, 5 % Chlorite (Chl), 3 % Muscovite, 1 % Opaque. Also, there can be observed some calcite veins.

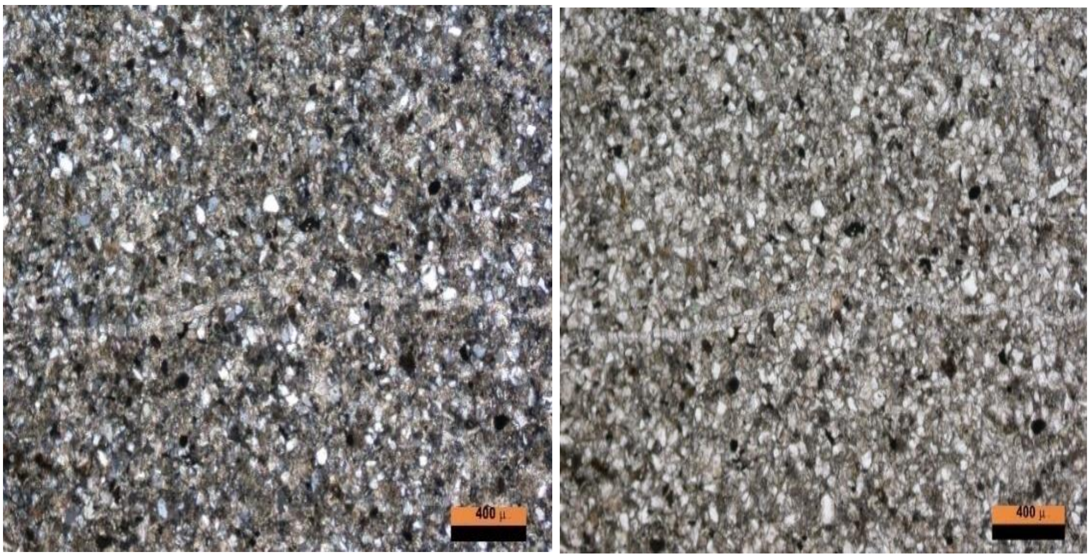

Figure 3.2.3: Sample 4, photomicrograph, cross polarized light, plane polarized light.

The very fine sandstone contains mainly quartz grains (Q), that are less than 0.1 mm in diameter and thin mica flakes including biotite and muscovite. Muscovite (M) is more abundant with bright colors, seen under cross polarized light. Clay matrix, dark brown in color, is subordinated to the component of siltstone. The sorting is well. The ratios of minerals are 40 % Quartz, 45-50 % Calcite, 2-3 % Opaque, 5 % Muscovite, 2-3 % Chlorite. Also, there are calcite veins.

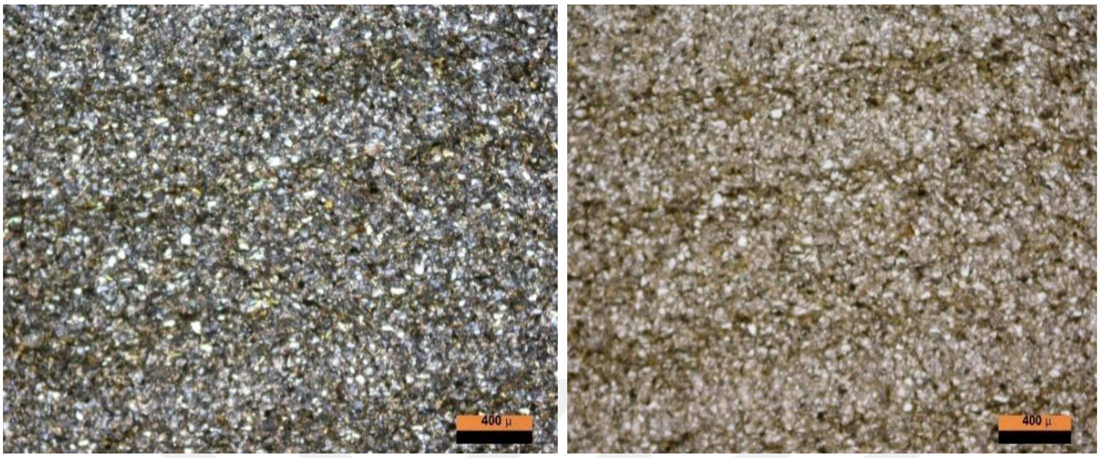

Figure 3.2.4: Sample 37, photomicrograph, cross polarized light, plane polarized light.

The sandstone is laminated, with laminae being defined by changes in grain size. The sorting of grains changes from laminae to laminae, but in larger grain laminae, the coarser sand grains always contain the smaller grains between the large one. The very fine sandstone contains mainly quartz grains (Q), that are less than 0.1 mm in diameter and thin mica flakes including biotite and muscovite. Muscovite (M) is more abundant with bright colors, seen under cross polarized light. Micritic carbonate matrix, dark brown in color, is subordinated to the component of siltstone. The sorting is well. The ratios of minerals are 55-60 % Quartz, 15 % Feldspar, 2-3 % Opaque, 20 % Muscovite.

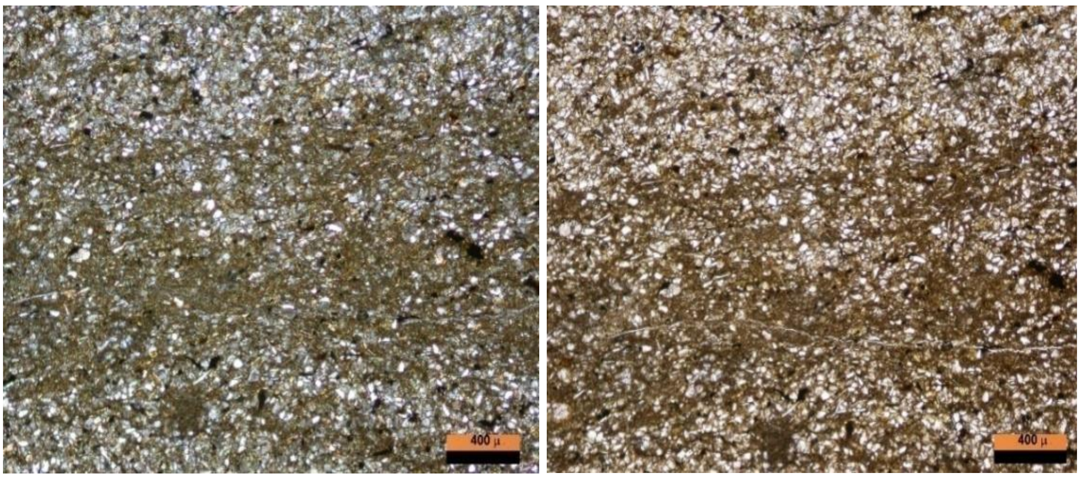

Figure 3.2.5: Sample 50, photomicrograph, cross polarized light, plane polarized light.

The shale is laminated, with laminae being defined by changes in grain size. The sorting of grains changes from laminae to laminae, but in larger grain laminae, the finer siltstone grains always contain the smaller grains. The very fine shale contains mainly quartz grains (Q), that are less than 0.05 mm in diameter, and chlorite, and opaque. Micritic carbonate matrix, brown in color, is subordinated to the component of siltstone. The sorting is well. The ratio of chlorite is 10 %.

The shale is laminated, with laminae being defined by changes in grain size. The sorting of grains changes from laminae to laminae, but in larger grain laminae, the finer siltstone grains always contain the smaller grains. The very fine shale contains mainly quartz grains (Q), that are less than 0.05 mm in diameter, and chlorite, and opaque. Sparitic calcite matrix, grey in color, is subordinated to the component of siltstone. There is the high degree of diagenesis. The porosity is very low and the sorting is moderately good. The ratios of minerals are 40-45 % Quartz, 25 % Calcite, 10 % Muscovite, 10 % Feldspar, 5-6 % chlorite, 2 % opaque.

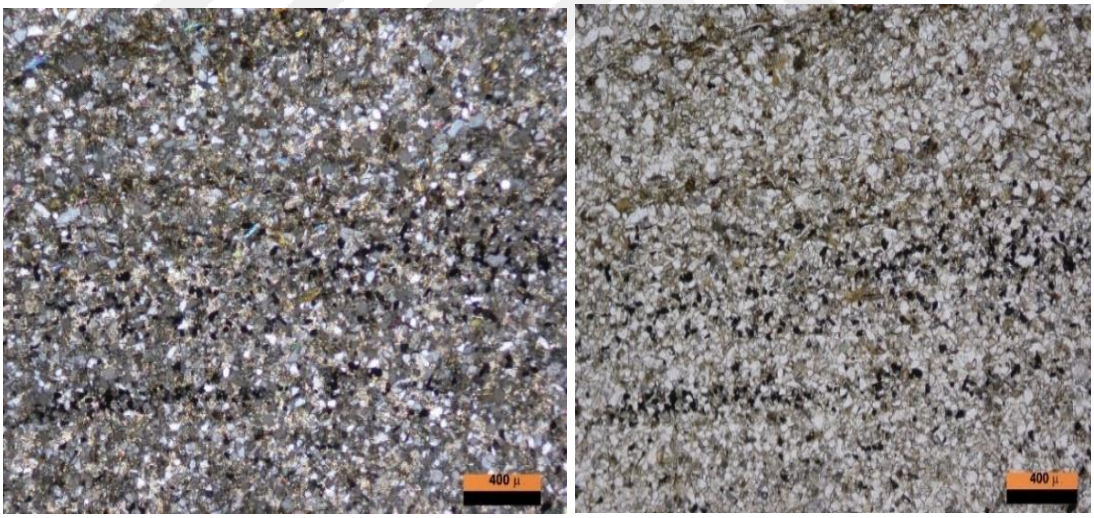

Figure 3.2.6: Sample 66, photomicrograph, cross polarized light, plane polarized light.

The very fine shale contains mainly quartz grains (Q), that are less than 0.05 mm in diameter, and chlorite, muscovite. Sparitic calcite matrix, grey in colour, is subordinated to the component of siltstone. There is the high degree of diagenesis. The porosity is very low and the sorting is well. There is a lamination of muscovite. The ratios of minerals are 55 % Quartz, 10 % Calcite, 20 % Muscovite, 15 % Chlorite. The age of sample is Eocene.

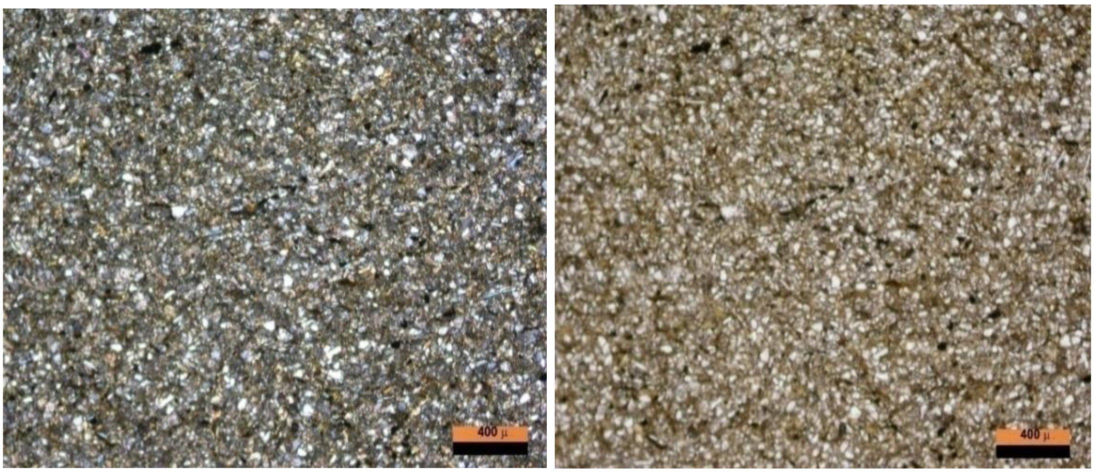

Figure 3.2.7: Sample 43, photomicrograph, cross polarized light, plane polarized light.

The shale is poorly laminated. The sorting of grains is well; the grains of the sample is close to shale. The very fine shale contains mainly quartz grains (Q), that are less than 0.05 mm in diameter, and chlorite, and opaque. Sparitic calcite matrix, grey in color, is subordinated to the component of siltstone. There is the high degree of diagenesis. The ratios of minerals are 50-60 % Quartz, 15 % Muscovite, 10 % Feldspar, 10 % chlorite, 5 % opaque.

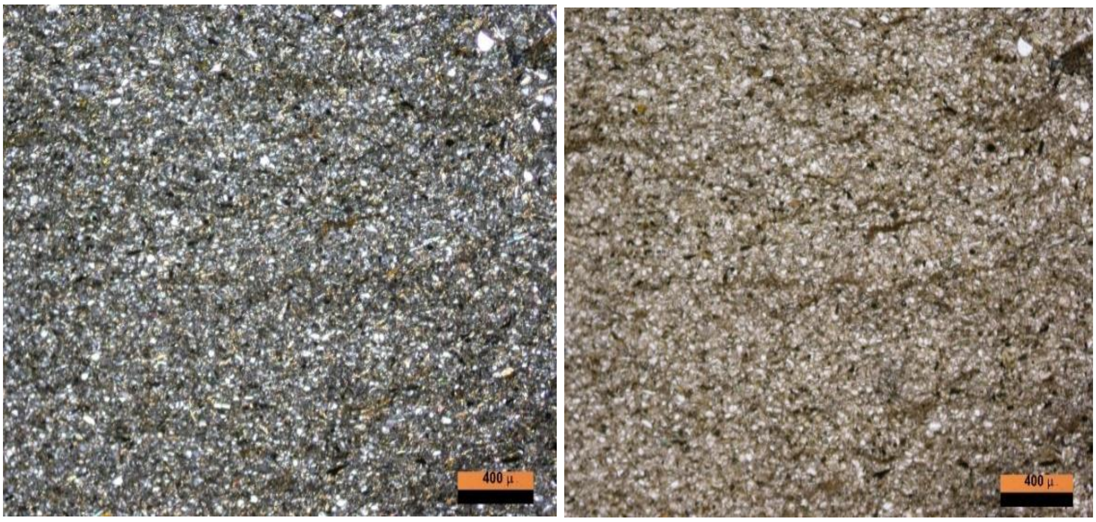

Figure 3.2.8: Sample 33, photomicrograph, cross polarized light, plane polarized light.

The shale is laminated, with laminae being defined by changes in grain size vertically. The sorting of grains is well; the finer siltstone grains always start to become to the fine grained sandstone. The fine shale contains mainly quartz grains (Q), that are less than 0.1 mm in diameter, and chlorite. Recrystallized micritic calcite matrix, grey in color, is subordinated to the component of siltstone. There are also calcite veins. The porosity is very low and the sorting is moderately good. The ratios of minerals are 40-45 % Quartz, 25 % Calcite, 10 % Muscovite, 10 % Feldspar, 5-6 % chlorite, 2 % opaque. It is a transition from Eocene age (Eoc) to the Oligocene age (Olg).

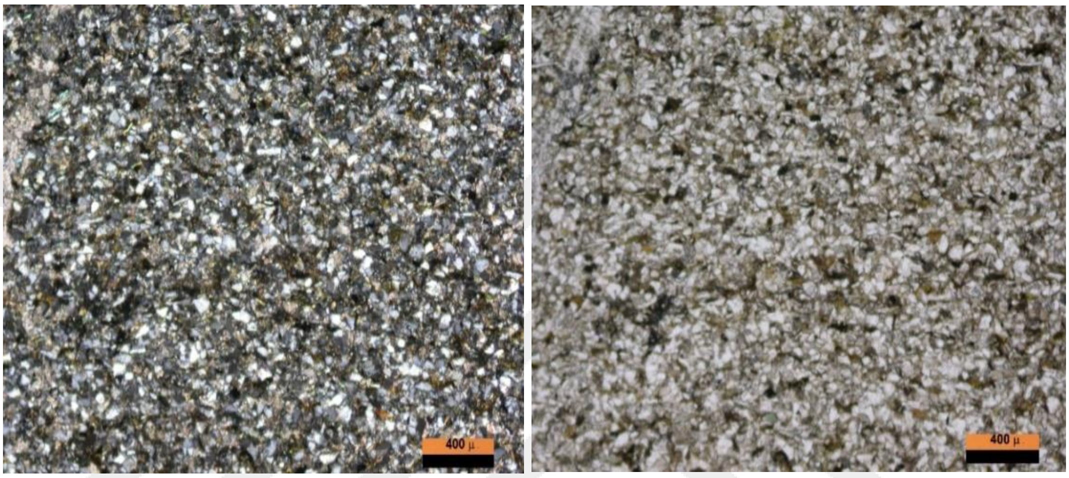

Figure 3.2.9: Sample 46, photomicrograph, cross polarized light, plane polarized light.

3.2.2 Detrital mineral composition

The Eocene and Oligocene aged sandstone and shale samples are composed of the three main constituents, quartz, feldspar, lithic fragments. Each grain group and its constituents are discussed below.

Quartz

The quartz constituents are monocrystalline and polycrystalline quartz and about 50% - 60% in total sandstone volume. Monocrystalline quartz (mQ) is commonly rounded to very rounded with grain sizes varying from 0.1 mm to 0.5 mm in diameter. Some quartz grains are in undulate extinction; which individual quartz grain appears black sweeping extinction when the microscope stage is rotated under cross polarized light (Figure 3.2.2). It is a result of strain and is found in quartz grains weathered from igneous rocks (Adams et al., 1988). Rarely the margins of some of the quartz grains are embayed (Figures 3.2.1 and 3.2.4). This is a result of corrosion of quartz from a volcanic origin in the investigated sandstones. The surfaces of some quartz grains are overlain by authigenic quartz in the form of overgrowth and syntaxial overgrowth (Figures 3.2.5, 3.2.7 and Figure 3.2.8). The original quartz surfaces are seen by a dark rim in polarized light. If the overgrowth is well developed, the overall shape of the quartz grain has changed from well-rounded to subeuhedral and euhedral, as a result of diagenesis.

Polycrystalline quartz (pQ) grains with prominent sizes of 0.1 mm to 1 mm in diameter are subrounded to very rounded. Most polycrystalline quartz grains are composed of several crystals. The contacts between the sub-grains are sutured and aligned (Figure 3.2.9). Probably, the quartz is originated from igneous fragments.

Feldspar

The feldspar grain group consists of sodium-calcium feldspars (plagioclase), alkaline feldspars and potassium feldspars (microcline, K-feldspar). Alkaline and K-feldspar are more abundant. Feldspars are important framework grains of the sandstones, but much less abundant than quartz accounting only for 5 % up to 15 % volume. Most feldspar grains are elongated, sub-spheroidal and rounded. Feldspar grains are less stable compared to quartz and rock fragments consisting principally of quartz. Therefore, most of them are altered and replaced by authigenic minerals and dissolved along the contact boundaries due to increasing pressure in burial stage. The solutions are precipitated in pore spaces (Figure 3.2.6). Plagioclases (Plg) are recognized by multiple twinning, some of them are

replaced by calcite (Figures 3.2.2), while microcline (Mi) and K-feldspar (F) are easily identified from the perthite and cross – hatched twinning (Figure 3.2.6). The feldspar grains which are drastically dissolved sometimes show only the remained feldspar rinds (Figure 3.2.8). This solution leads to forming of micro pores within them. Some K-feldspar grains are also replaced by calcite (Figure 3.2.1), and only some feldspar specks are remained. Locally the K-feldspar grains are completely replaced by calcite, so that they are not easy to recognize by the typical feldspar features.

Lithic fragments

Rock fragments are important components of the sandstones. The rock fragment volume in the sandstones is about 15 % - 25 %. The lithic fragments are volcanic clasts, igneous and sedimentary rock fragments. The sedimentary lithic fragments with subangular and angular shape contain very fine grains and are less common. The clasts (Chert) are round (Figure 3.2.1) and made up of very fine-grained quartz (micro quartz), but some clasts are embayed at the margins. This has occurred as a result of corrosion of the clasts during diagenesis. The fragments of quartzite and igneous rocks in sandstones are rich in quartz. An alignment of quartz grains as in quartzite fragments is conjunction with deformation as witnessed by elongate polycrystalline quartz. The igneous lithic fragments consisting of principal quartz, feldspar and minor alkali minerals have previously undergone alteration due to auto hydrothermal reaction and feldspars have been subject to sericite alteration.

3.3 Diagenesis and Turbidite System

Diagenesis is a process in which sediments have undergone chemical and physical changes which occur during the formation of rocks from loose sediment after its deposition. The term "diagenesis" was introduced by Von Guembel in 1868 to describe sediment alterations that take place during post-depositional processes of lithification and has been used for a wide range of alterations that affect sediments during their progress to become sedimentary rocks (Twenhofel, 1939; Correns, 1950). It however does not include weathering.

Late Eocene coarse-grained turbidite system and its landward equivalents constitute deposits. It is a third-order depositional sequence (Mitchum et al., 1977) and comprises the oldest sediments of the studied interval. In lithostratigraphic nomenclature (Figure 3.3) (Turgut et al, 1987; Siyako, 2006), it composes the upper part of the Hamitabat Formation, which is made up of mostly the alternation of sandstone and shale beds deposited in various environments from deep to shallow marine. Sequence-1 is dated as Late Eocene on the basis of planktonic foraminifers (Erenler, 1987; Ediger et al., 1998). The turbidite system is underlain by two major substrata; pre-Tertiary metamorphic rocks of the Istranca Massif and Lower to Middle Eocene siliciclastic unit. Metamorphic rocks of the Istranca Massif are composed of pre-Triassic basement rocks and the overlying Triassic-Jurassic age metasedimentary rocks (Pamir and

Baykal, 1947; Çağlayan et al., 1988; Üşümezsoy, 1990; Okay and Yurtsever, 2006). They are exposed to surface from Çatalca near Istanbul to the Bulgaria territory in a 200 km long (east to west) and 25-30 km wide (north to south) zone (Okay and Yurtsever, 2006). Pre-Triassic part was metamorphosed in amphiobolite and high-grade green schist facies, and cut by the Paleozoic granitoids. The overlying terrestrial and shallow marine Triassic and Jurassic sedimentary rocks were metamorphosed and deformed in compressional regime in Late Jurassic and Early Cretaceous in green

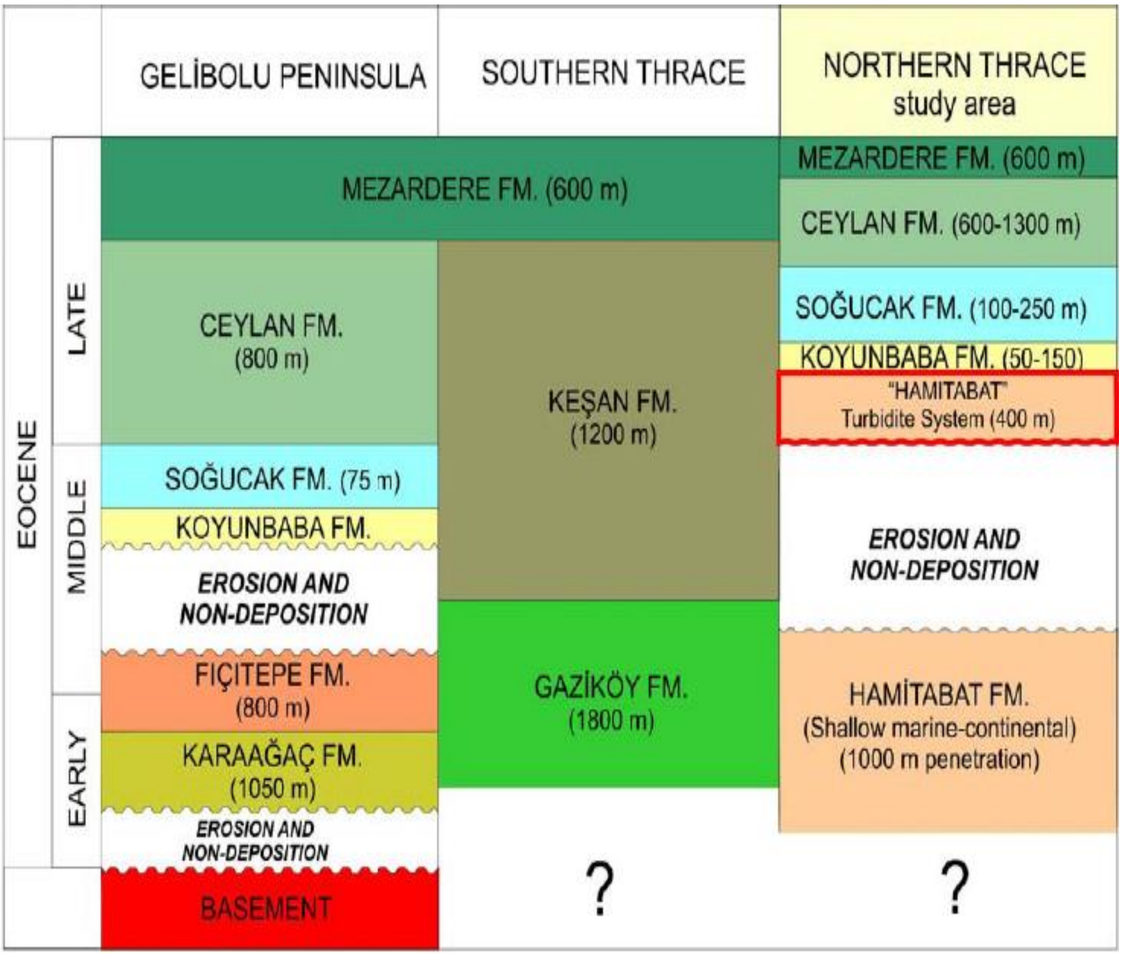

Figure 3.3: Stratigraphic relations of the Eocene formations in the Gelibolu Peninsula. Southern Thrace and Northern Thrace (Siyako, 2006).

schist facies (Pamir and Baykal, 1947; Çağlayan et al., 1988; Üşümezsoy, 1990; Okay and Yurtsever, 2006). This type of basement rocks was penetrated by most of the wells along the northern margin of the basin. Second type of substrata is the Lower to Middle Eocene siliciclastic unit. They compose the lower part of the Hamitabat Formation and its depositional environment varies from terrestrial to shallow marine.

A turbidite system is defined as a body of genetically related massflow and turbidity current facies and facies associations that were deposited in virtual stratigraphic continuity (Mutti and Normark, 1987, 1991). Shanmugam (2000) also states that the classification of sediment gravity flows into Newtonian flows (e.g. turbidity currents) and plastic flows (e.g. debris flows) based on fluid rheology and flow state is a meaningful and practical approach. The Figure 3.3.1 depicts the major elements of a turbidite system in a three-dimensional model. Like many other turbidite systems, facies and geometry of the studied turbidite system were affected by the changing basin floor morphology instead of a uniform basin floor. The terms; ponded turbidites (Van Andel and Komar, 1969; Prather et al., 1998), contained turbidites (Pickering and Hiscott, 1985) and/or confined turbidites (Lomas and Joseph, 2004) have been used to characterize sediment gravity flows and their deposits which fill the floor of an enclosed depression area (mini basin, sub basin, ponded basin) and are unable to surmount the bounding slopes. Studied turbidite system was analyzed in three major depocenters based on their own sediment delivery pathways, areal extent and facies architecture.

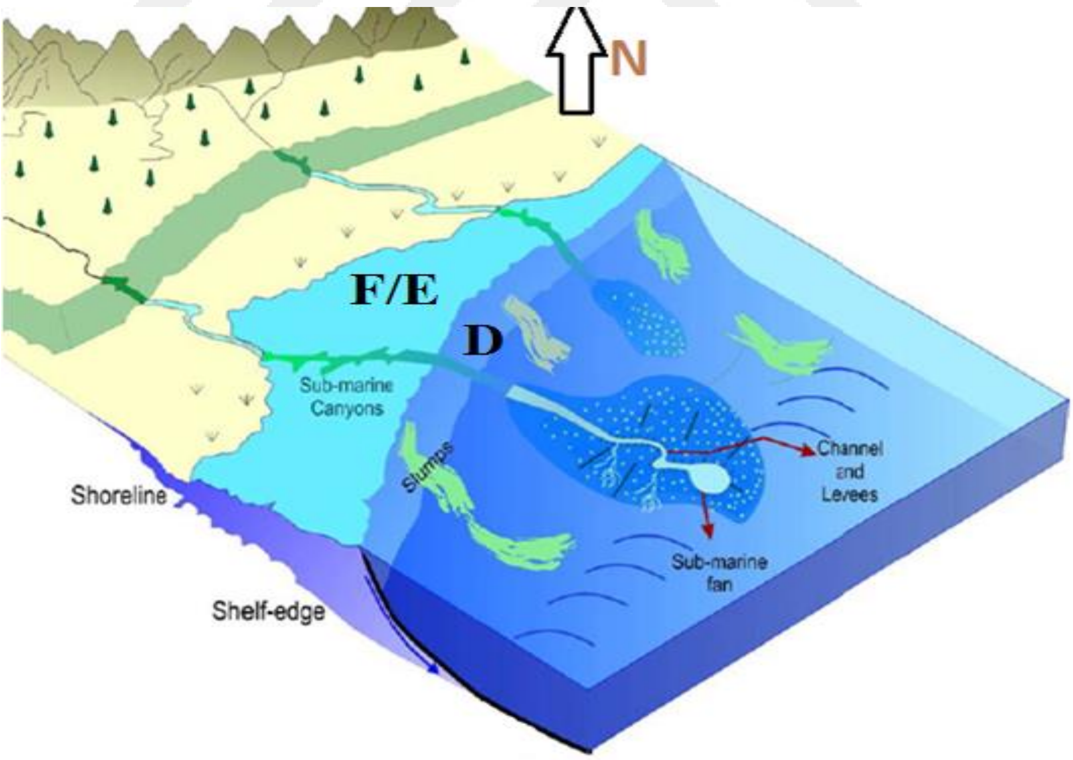

Figure 3.3.1: The figure depicts major elements of a turbidite system in a three-dimensional depositional model (redrawn from Mutti and Normak, 1991)

3.3.1 Cement and authigenic minerals

In the herein investigated samples, cement and authigenic minerals are mostly present in all the sandstones and mainly consist of calcite, anhydrite and authigenic quartz, albite, clays and hematite. The cement volume is between 10 % and 30 %. Calcite cement is volumetrically dominant in most of sandstones.

Iron oxides

Hematite or a mixture of hematite and clays are almost omnipresent in the studied sandstones. Hematite occurs as a skin on grain surfaces. The presence of hematite is observed from microscopic investigations. Hematite directly precipitates on the grain surfaces, visible as dark – brown rims on grain surfaces. This suggests that the formation of these grain coatings occurred in the early diagenesis or in eogenesis under the presence of oxygen. In this stage, the chemistry of the interstitial waters was mainly controlled by the depositional environment as demonstrated by Schmidt et al., (1979). As demonstrated in figures, the thick hematite skins on corroded grains and hematite staining of clastic grains could result from weathering processes. Iron was released during the breakdown of unstable ferromanganese or iron oxide minerals in the sandstones under surface temperature and pressure conditions. Additionally, iron was probably transported into the basin by meteoric waters from weathering of the adjacent areas and precipitated under favourable oxic conditions.

Clay minerals

Clay minerals are ubiquitous in all the sandstones. The most predominant authigenic clays are illite and chlorite, which occur in a number of morphologies in the form of clay coatings on detrital grains and as pore – filling. Smectite is locally present in minor amounts.

İllite - smectite

Illite occurs in distinct forms as grain - tangential illite coatings, pore – filling and pore - bridging illite ribbons. Illite coatings are commonly stained by hematite forming dark–red rims surrounding detrital grains, as seen in thin sections. According to Walker, (1976), the grain-coating illite and staining by hematite are typical for the red beds in Rotliegend sandstones. These coatings are predominant filamentous illites probably precipitated from pore water due to supplying of meteoric water into subsurface. Illite–smectite is present in a small fraction in the form of thin fibres as flakes. The pore–filling and pore - bridging illite ribbons could have been commonly formed later in the burial phase. The illites are

linked to extensive grain dissolution, as feldspars, volcanic fragments. Sometimes, illite filaments are released from surfaces at the cost of the authigenic albite, where albite is replaced by illite. Generally, the appearance of illite and illite–smectite together with authigenic chlorite can complicate the geometry of pore networks and the high resistance to fluid flows through the sandstones, causing a reduce of the permeability.

Chlorite

Authigenic chlorite is present in some the studied sandstone samples. The chlorites with irregular morphology mix with illite forming grain coatings. Individual chlorite crystals with euhedral and subeuhedral shapes arranged in rosette pattern are approximately 5 – 15 μm in diameter and less than 1 μm thick. They are perpendicular to the detrital grain surfaces facing into the pore space. This suggests that the chlorites were formed in the early diagenetic process (eogenesis) as reported by Hayes (1970) and Humphreys et al. (1989). The studies show chlorite in form of grain coatings which can precipitate early in diagenesis, but before the onset of metamorphism or weathering. The form of chlorite with subeuhedral crystal plates is present in pore filling cement. Sometimes the illite-chlorite with small and thin platelets, as flakes, is found in the void filling between the grains. Probably, the chlorites formed in the burial stage. In this buried diagenesis, the elements Al and Si were released from many dissolved detrital grains and Fe and Mg were supplied from the breakdown of ferromagnesian minerals in the rock fragments and matrix components into pore waters. These formed then the fluid sources to crystallise the authigenic chlorites. The chlorites can be directly precipitated from the pore fluids as investigated by Humphreys et al. (1989). The authigenic grain coating chlorites formed in the early diagenesis, while the pore filling chlorites formed in the burial diagenesis.

Authigenic quartz

Quartz cements are less abundant than calcite and precipitate in distinct forms. Authigenic quartz occurs in the form of overgrowth and syntaxial overgrowth on the quartz grain surfaces with sharp crystal edges. The authigenic quartz with perfect crystal habits has been growing quartz framework surfaces and into pore spaces. The authigenic quartz overgrew the outer rim of clay minerals and/ or hematite skin which separated the quartz frameworks and the authigenic quartz. The overgrowth and syntaxial quartz are overlapped by calcite in pore filling cement. This indicates that the first generation cement constitues clay minerals and/ or hematite coatings and subsequently the authigenic quartz which formed followed by calcite cement. The overgrowth and syntaxial quartz precipitation are possibly connected to meteoric waters, which took up SiO2 released from dissolution and chemical weathering processes of less stable minerals. Quartz cement with large crystals in the form of pore – filling precipitates most likely during burial diagenesis or in mesogenesis phase, as quartz cement formation is a significant process only at temperatures greater than about 700-800°C (Choquette et al., 1970). In general, the authigenic quartz can significantly reduce the size of intergranular pores and pore-throats, leading to a considerable reduction of porosity and permeability of sandstones. Locally, authigenic cristobalite druses with rhomboidal morphology scatter on clay layers in pore spaces. The cristobalite crystals also precipitated from the SiO_2 rich pore fluids as did the authigenic quartz but the cristobalite crystallizes in higher temperature than the authigenic quartz. In the burial diagenesis, the increasing temperature was responsible for the formation of cristobalite.

Authigenic Feldspar

Authigenic feldspar is known as common cement formed during diagenesis. It forms overgrowths on detrital grains or as pore filling cements. Authigenic albite occurs as a partly throat blocking and pore-filling crystal. The albite grows outer clay mineral coatings indicating that it formed after these clay mineral coatings. The albite is precipitated in the early diagenesis due to the sodium dominated formation water. Subsequently, widespread during burial diagenesis authigenic feldspar occurs as overgrowths on detrital grain surfaces. A possible reason for the albite formation is that Al ions which were released from partial dissolved detrital grains re-precipitated at crystallization nuclei, at favourable diagenetic conditions.

Halite

Authigenic cubic halite crystals preferentially precipitate and scatter across clay coatings. They only locally occur in a couple of the sandstones investigated. Probably the halite crystals can be associated with evaporitic conditions or that a mixture of ground water and brines derived from the overlying Zechstein sequence where the halite could form in the early diagenesis but after the clay coatings.

Calcite

Calcite is one of the most abundant cements in sandstones. Calcite typically occludes pore spaces, but also partly replaces detrital feldspars and volcanic rock fragments. Calcite formed during early diagenesis and continued during burial diagenesis. The calcite shows complex textural relations to other diagenetic minerals. In the early diagenesis, calcite forms commonly as pore - filling cements, which precipitated directly on grain surfaces. Sometimes, overgrowth of calcite overlaps on the hematite – clay coatings, albite and quartz overgrowths. The calcite formed simultaneously sediment deposits in shallow water environment. In the burial diagenesis, calcite precipitates locally in pore spaces and replaces the dissolved feldspar grains and volcanic fragments. The calcite extracted from meteoric water, which primarily derived from the overlying Zechstein sequence and was supplied by marine pore waters due to the Zechstein marine transgression. The replacement only occurs at the depth below than 4900 m. It is possible that acidic fluids extracted from the underlying Carboniferous strata were responsible for the dissolution as investigations (Purvis, 1989; Purvis, 1992), where the sandstone deposits underlain the Westphalian coals and carbonaceous shales (Upper Carboniferous). However, a clear determination between calcites of the early and burial diagenesis was not possible for all samples as calcite tends to recrystallize and the textures are difficult to be recognized.

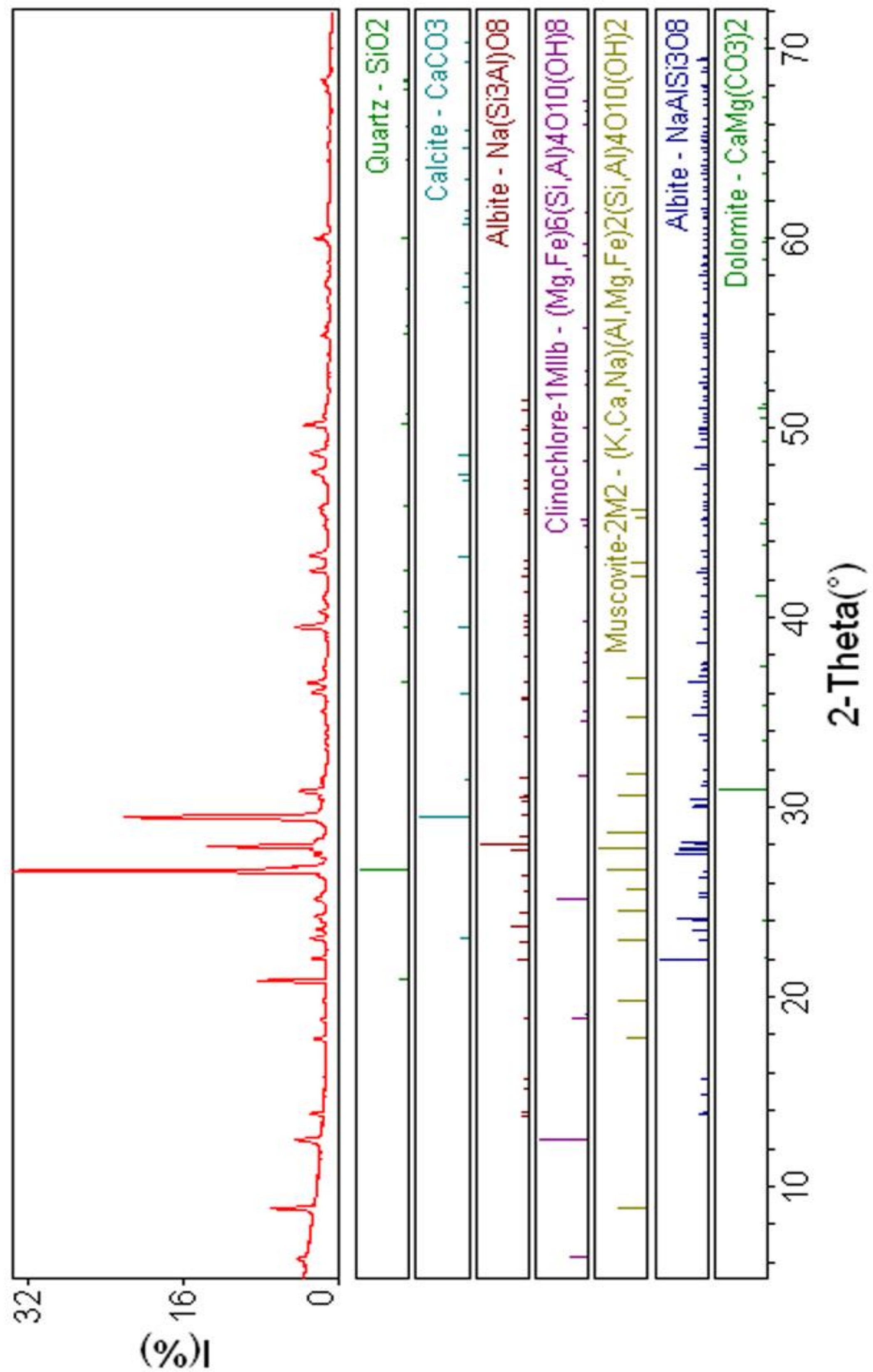

Figure 3.3.1.1: Sample 4 – Eocene aged Sandstone. The highest peak indicates the concentration of Quartz (Q), then other abundant minerals are chlorite, calcium strontium silicates, muscovite and halloysite.

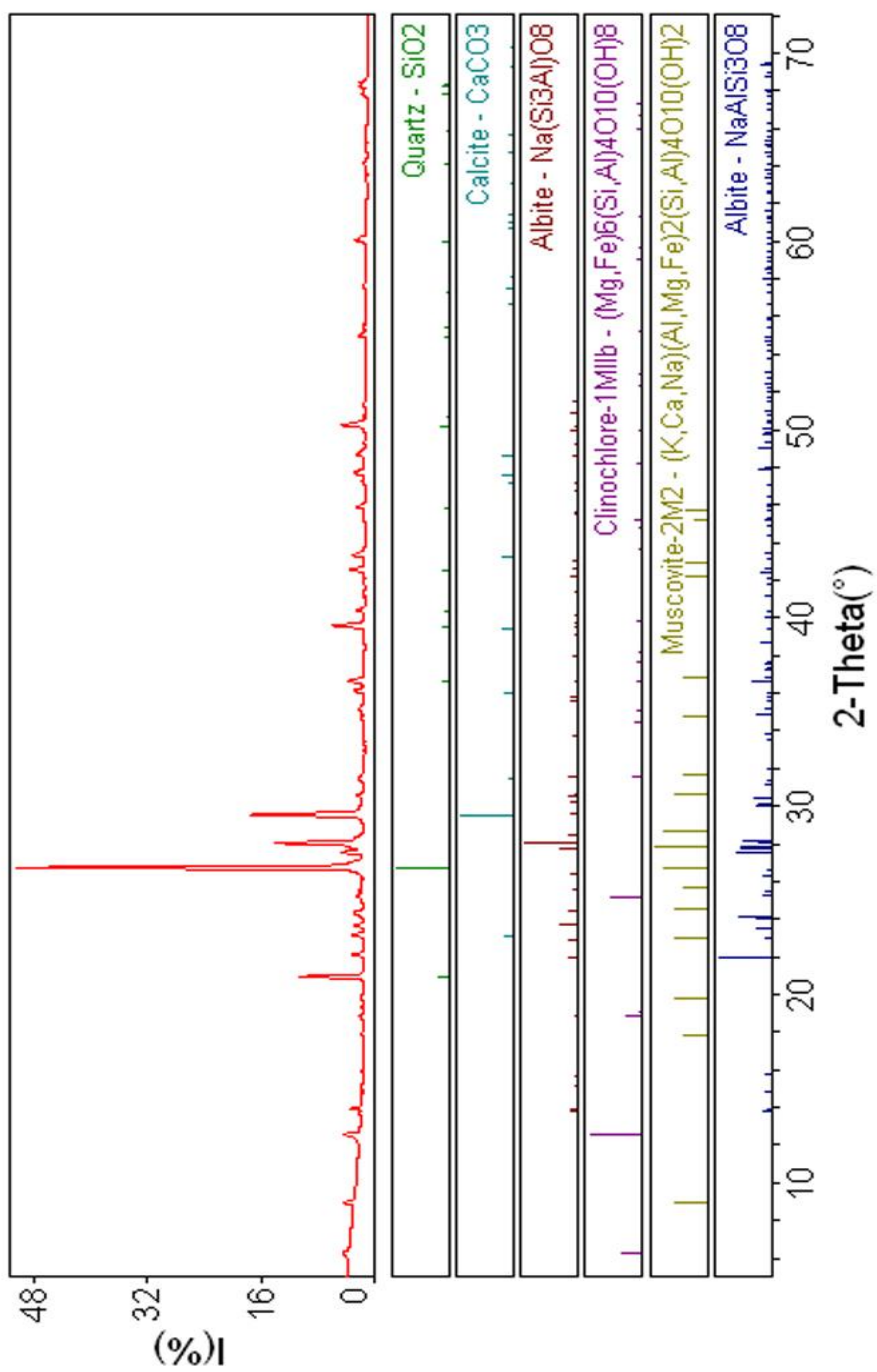

Figure 3.3.1.2: Sample 27 – Eocene aged Sandstone. The highest peak indicates the concentration of Quartz (Q), then other abundant minerals are chlorite, potassium beryllium silicates, muscovite and feldspar.

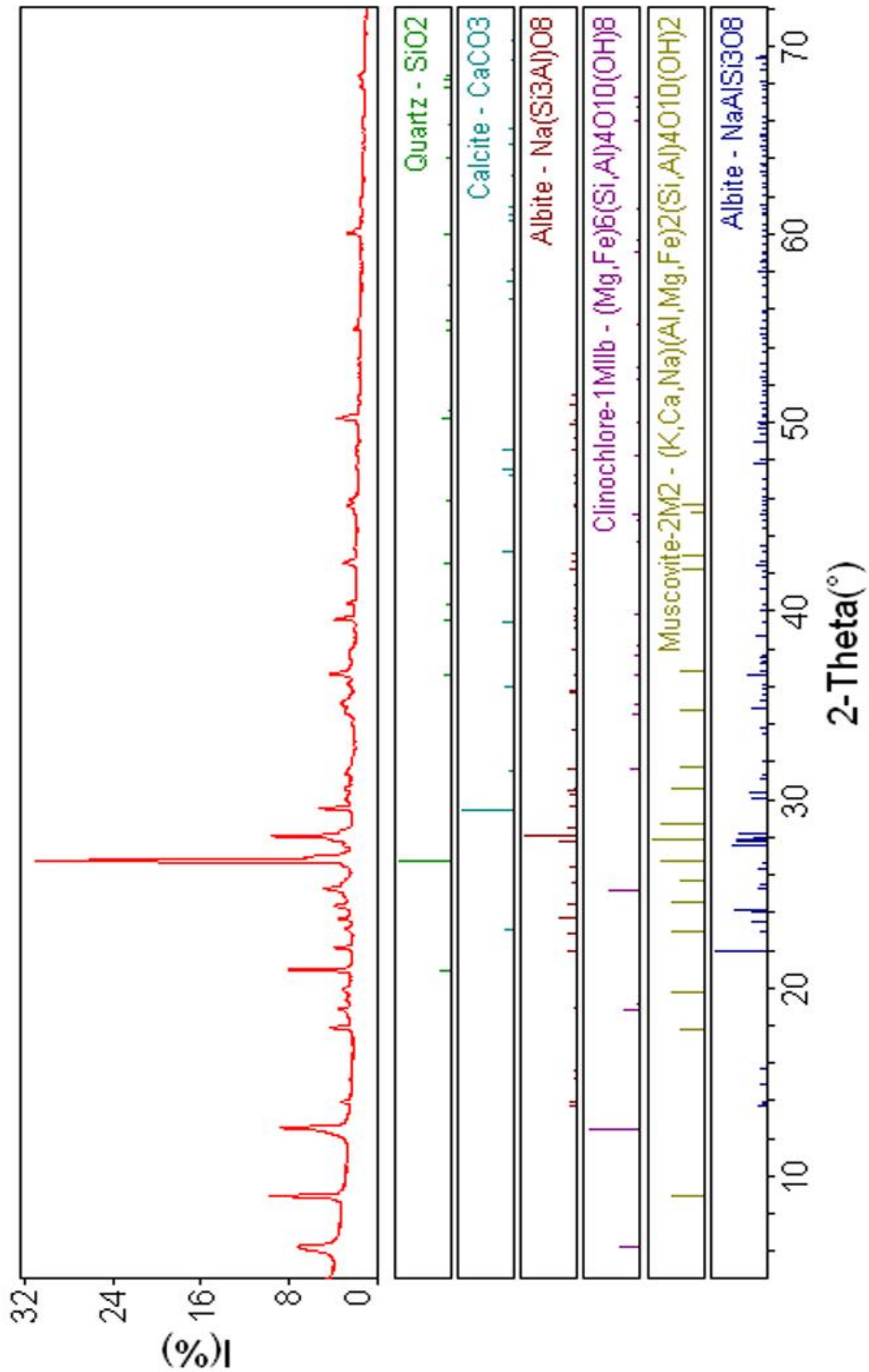

Figure 3.3.1.3: Sample 33 – Eocene aged Shale. The highest peak indicates the concentration of Quartz (Q), then other abundant minerals are chlorite, muscovite and feldspar.

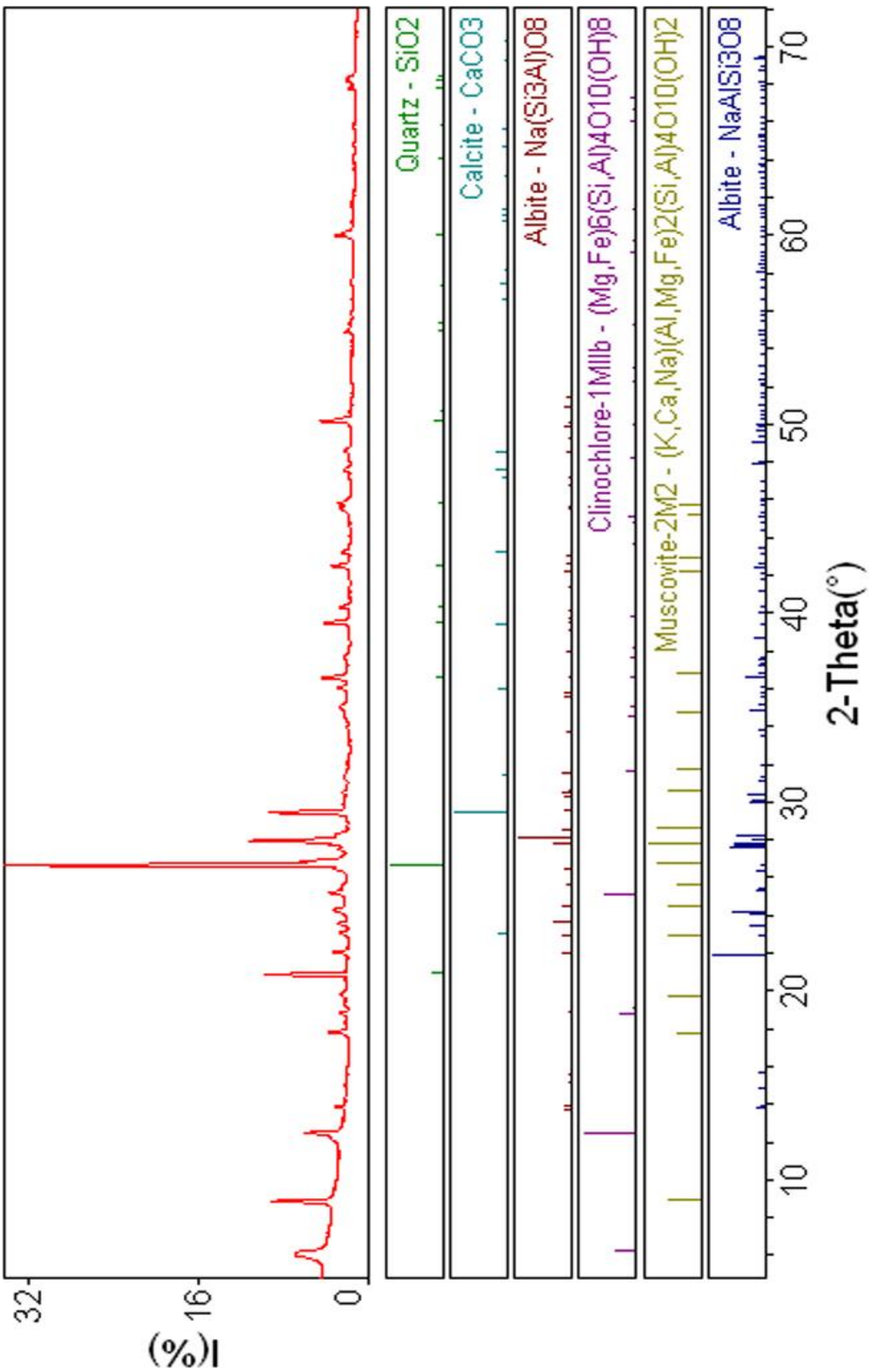

Figure 3.3.1.4: Sample 37 – Eocene aged Sandstone. The highest peak indicates the concentration of Quartz (Q), then other abundant minerals are chlorite, clay mineral montmorillonite, muscovite and feldspar.

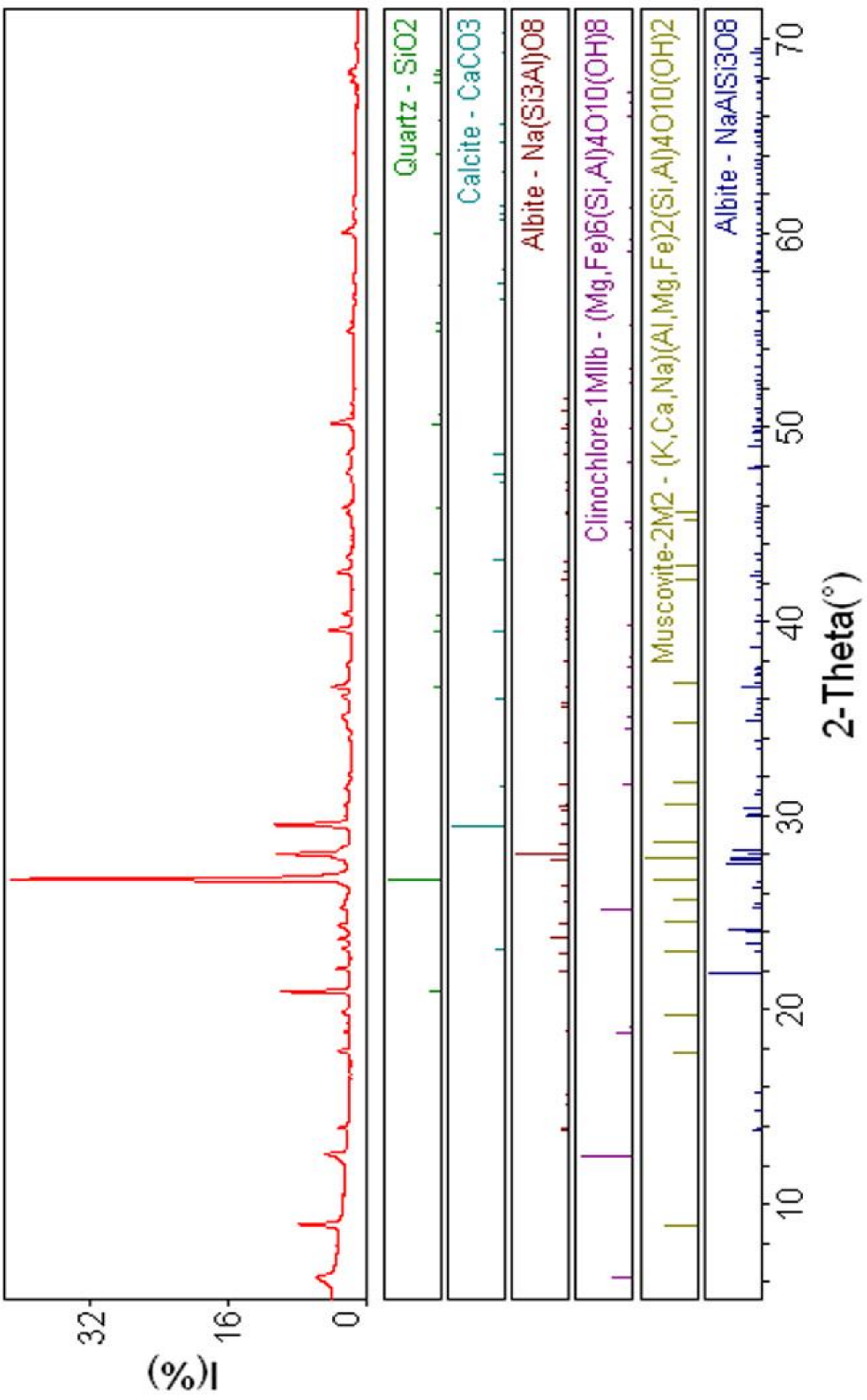

Figure 3.3.1.5: Sample 43 – Eocene aged Shale. The highest peak indicates the concentration of Quartz (Q), then other abundant minerals are chlorite, muscovite and feldspar.

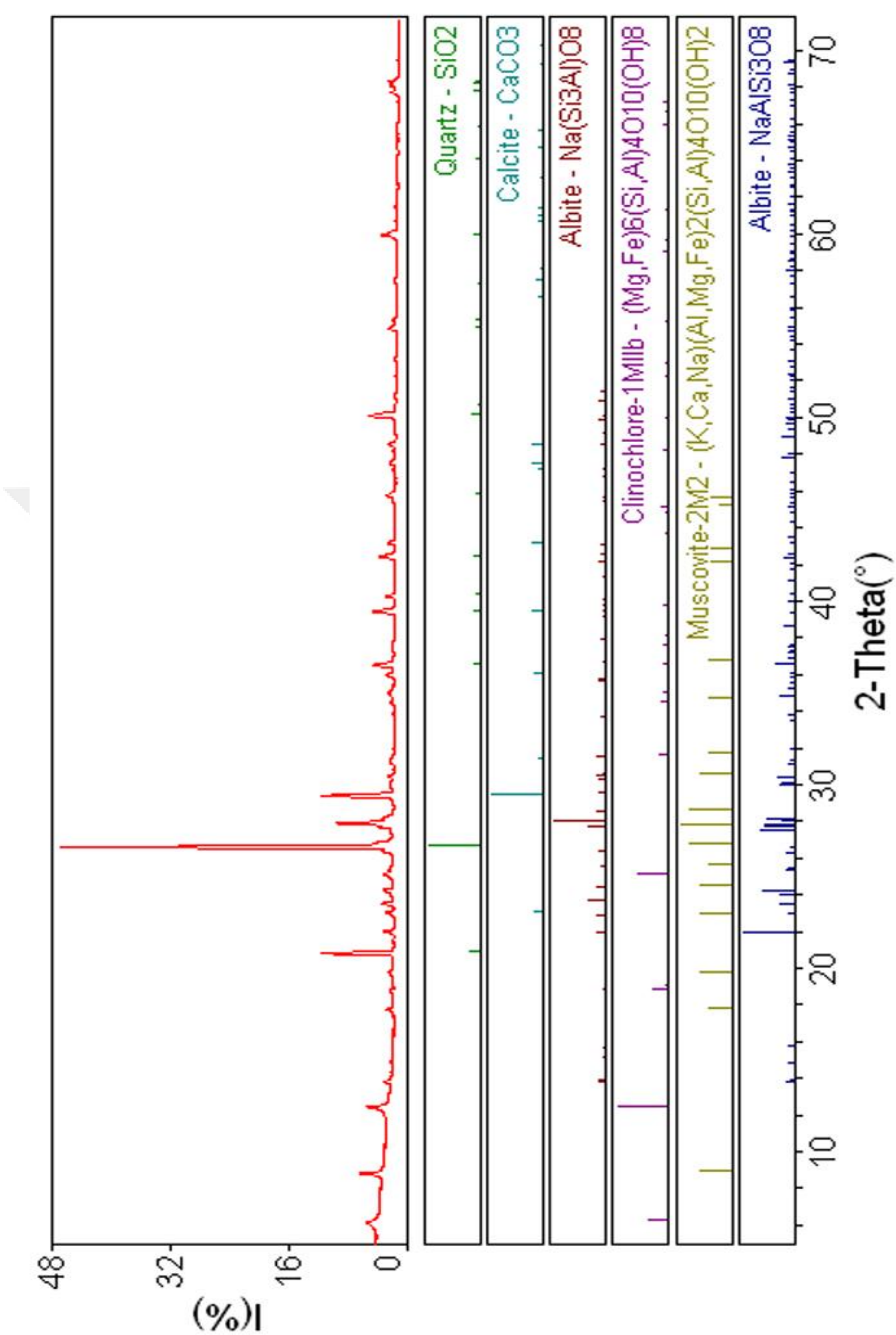

Figure 3.3.1.6: Sample 46 – Eocene aged – Oligocene aged Shale (transition sample). The highest peak indicates the concentration of Quartz (Q), then other abundant minerals are chlorite, muscovite and feldspar.

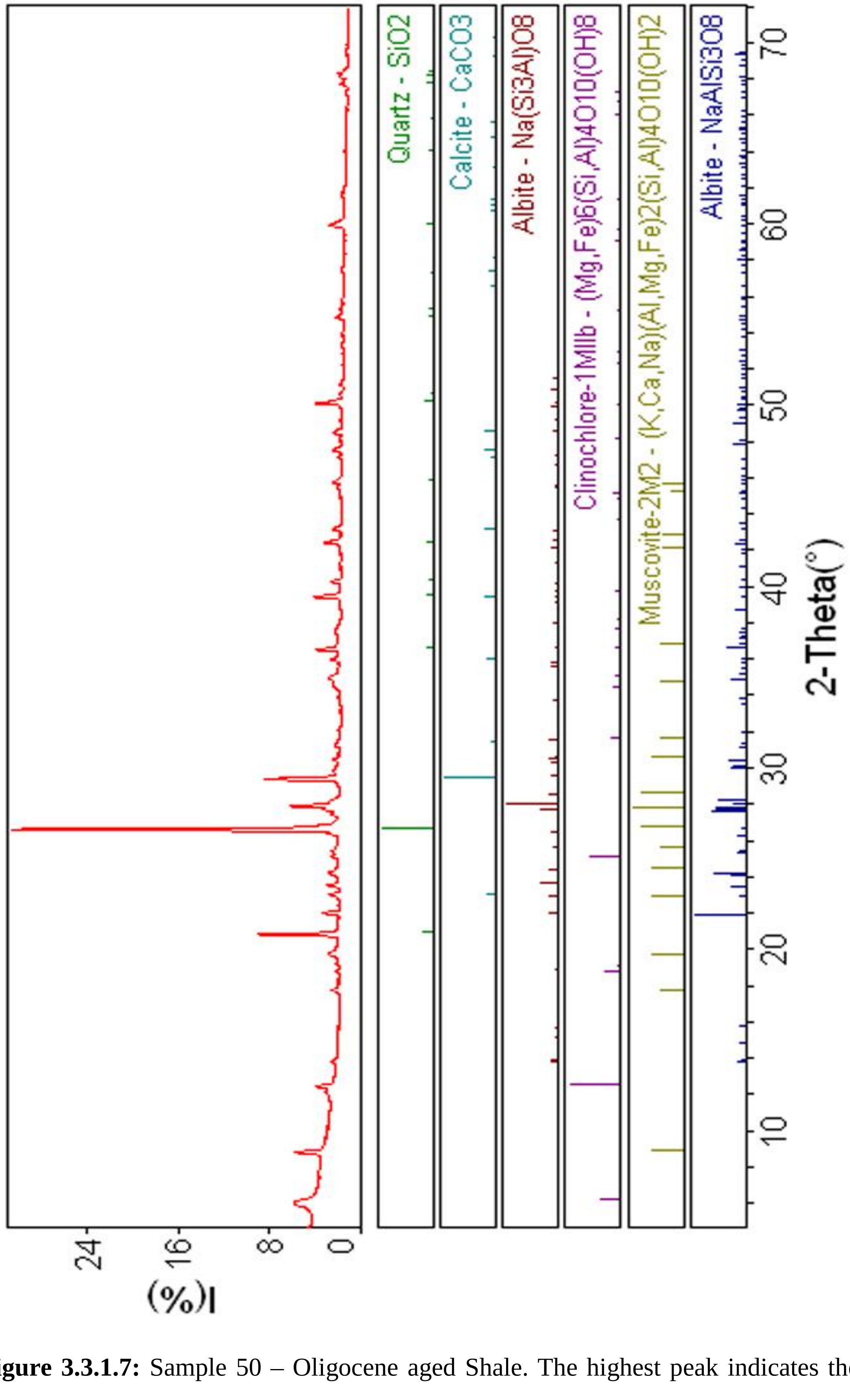

Figure 3.3.1.7: Sample 50 – Oligocene aged Shale. The highest peak indicates the concentration of Quartz (Q), then other abundant minerals are chlorite, muscovite and feldspar.

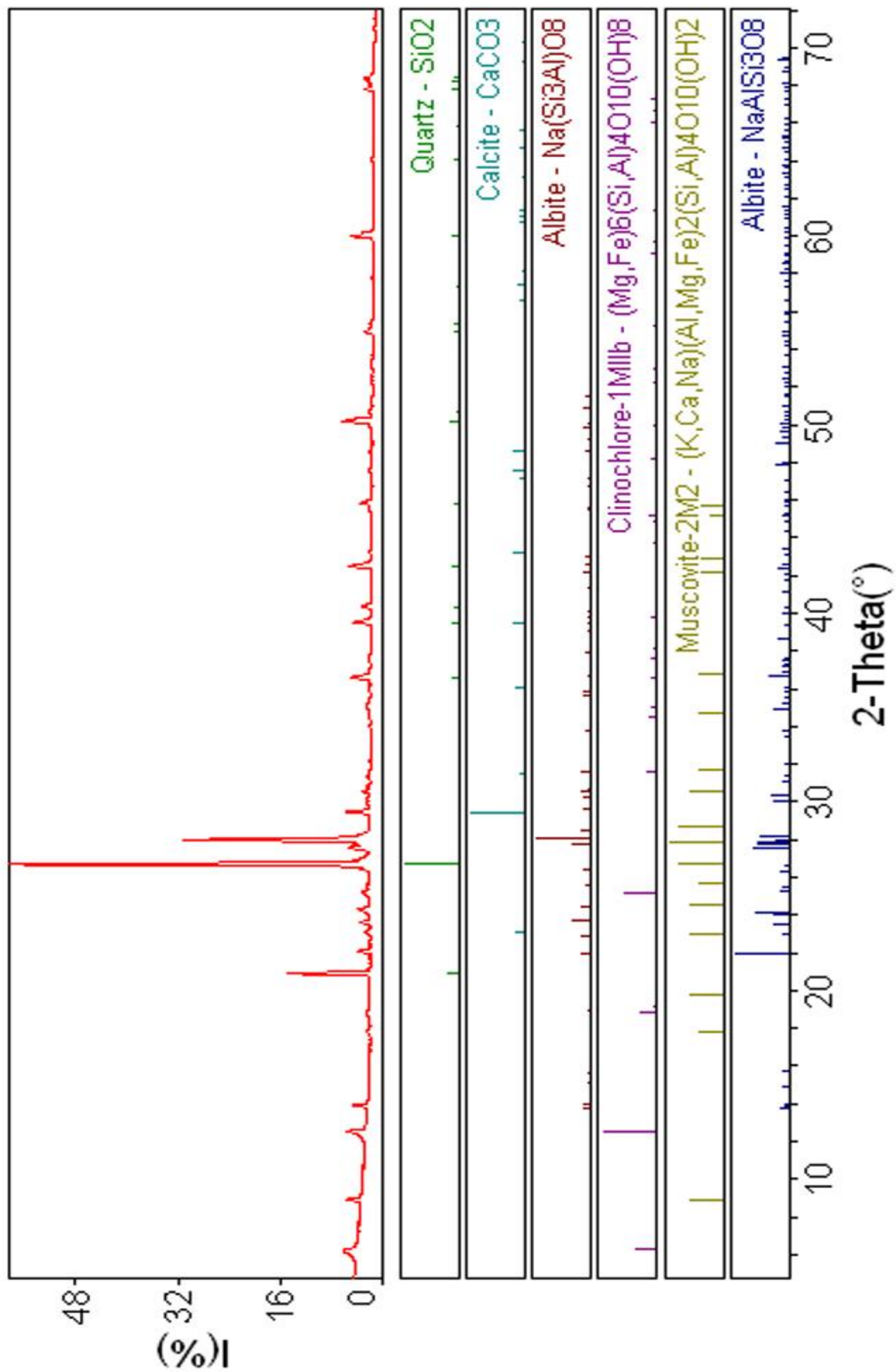

Figure 3.3.1.8: Sample 55 – Oligocene aged Sandstone. The highest peak indicates the concentration of Quartz (Q), then other abundant minerals are chlorite, muscovite and feldspar.

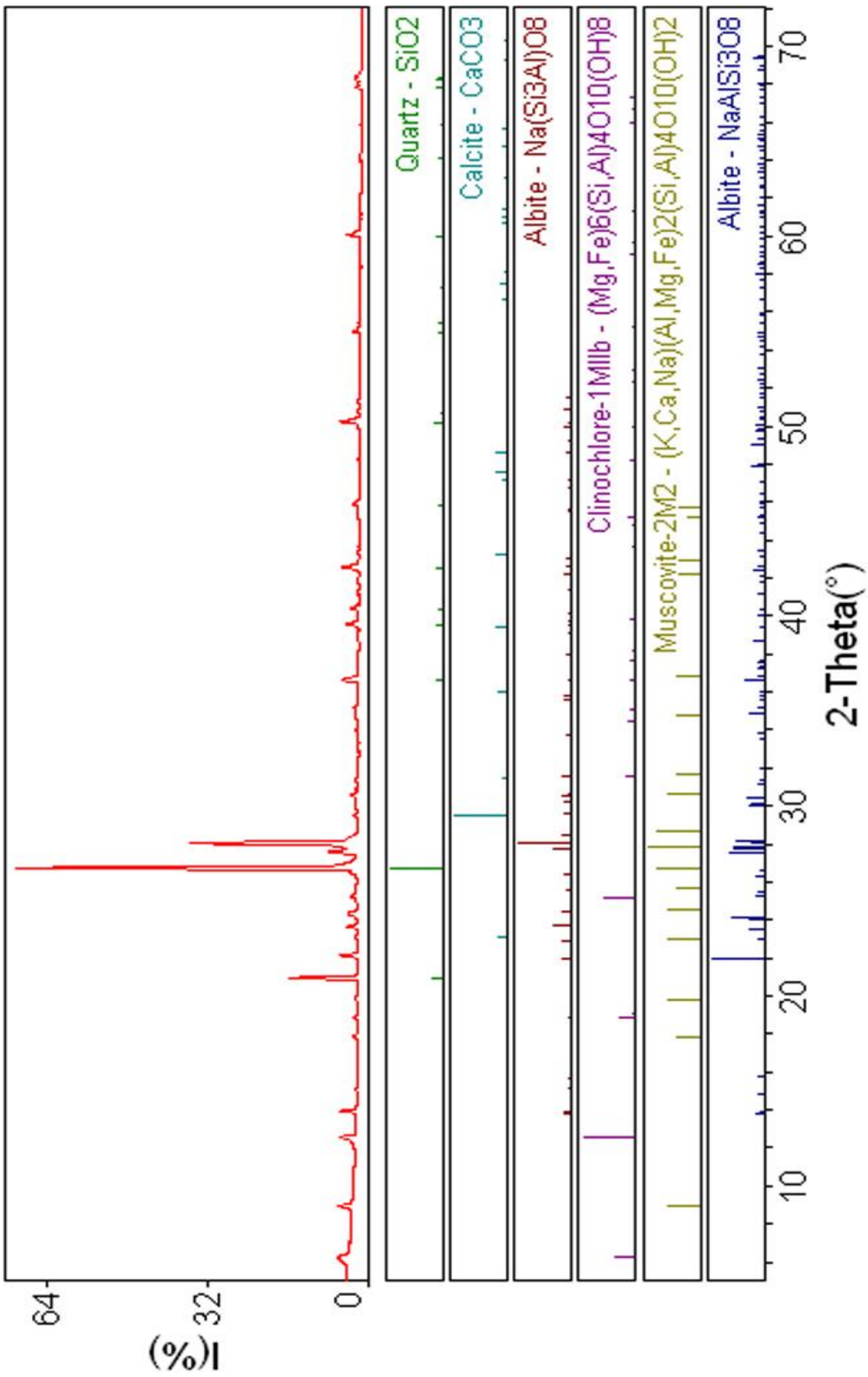

Figure 3.3.1.9: Sample 59 – Oligocene aged Sandstone. The highest peak indicates the concentration of Quartz (Q), then other abundant minerals are chlorite, muscovite and feldspar.

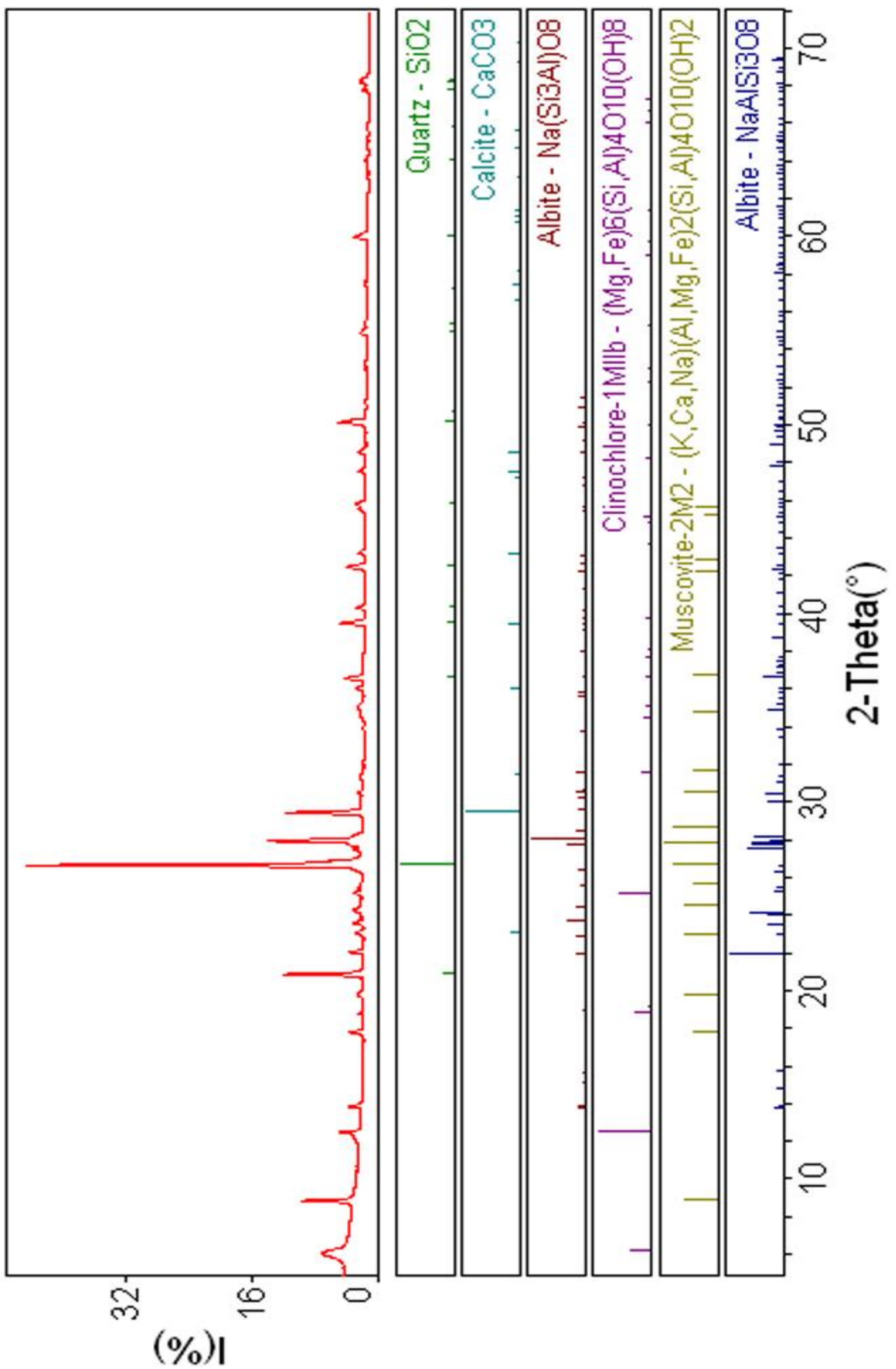

Figure 3.3.1.10: Sample 66 – Oligocene aged Shale. The highest peak indicates the concentration of Quartz (Q), then other abundant minerals are chlorite, muscovite and feldspar.

4. THE DIAGENESIS AND ASSOCIATION OF FACIES

Clay minerals in the early phase of diagenesis are predominantly smectite, which surrounds the grains and precipitated from pore waters. The cements in pore–fillings are commonly quartz, calcite, and albite. Quartz cements precipitated from silica-rich fluids which probably largely originated from fluvial settings. Smectite grain coatings were formed in continental deposits as in continental meteoric water (Wilson, 1992; Platt, 1994; Schöner, 2006). Also, the occurrence of calcite and carbonate cements shows that it is likely that cements precipitated from the overlying Zechstein evaporates (Purvis, 1992). Locally the precipitation of halite indicates that the water was increasingly saline. It is likely that authigenic albite was associated with sandstones of marine origin (Rasmussen et al., 1996) or invaded by marine brines and was trapped by Zechstein deposits (Purvis, 1989). Authigenic albite is largely widespread at burial depth, due to the fact that Na+ was released from extensively dissolved unstable grains, mostly feldspars and volcanic fragments. The dissolution was responsible for the crystallization of smectite and chlorite in pore - fillings. The latest cement is calcite, which precipitated in local pores and in pits of dissolved grains. It is possible that the fluids dissolved the unstable grains, forming smectite and chlorite in pores occurred in sandstones which were nearby or adjacent to the underlying Carboniferous sequence. The fluids derived from the Carboniferous deposits (Platt, 1991; Platt, 1993). The diagenetic alteration had a large impaction on the grain morphology and the pore geometry.

4.1 Diagenetic Relations

4.1.1 D Facies (Pelitic Arenaceous Facies 1)

This facies is very widely distributed in the study area. It forms a number of thick sequences, particularly in flysch of Eocene and Oligocene ages that forms part of the folded terrane and is noted by various formation of names. It is also developed, mostly in alternation with Facies C, throughout Gaziköy Formation. These deposits correspond to the “distal” facies of Walker (1967), but several reservations must be made in the use of this term.

The texture and structure of the arenaceous part as well as the predominance of the pelitic intervals indicate that relatively slow and dilute turbidity currents transported the entire sediment load in suspension. The coarsest fraction (fine-grained sand) of this sediment was deposited by traction, primarily under lower-flow regime conditions; sometimes, however, an initial upper-flow regime phase was present, as seen from the thick, flat laminae of interval. The fine fraction simply settled out of suspension without undergoing traction. Because the effects of traction could be accentuated or diminished according to the relation between rate of sedimentation, concentration of pelitic material (which influences the cohesion of the sediments just deposited), and the water content, a great variety of laminated structure, particularly oblique laminae, form in this deposits.

4.1.2 E Facies (Pelitic-Arenaceous Facies 2)

This facies are probably implied or hinted at to some degree by Walker (1965, 1967) who described Ta-Te sequences consisting of thin strata containing a graded interval that past directly upward to pelitic. Walker, however, considered them to be distal turbidities and included them with Tc-e sequences.

In the study area these facies to date has been recognized in the sandstone of the Keşan Formation. The origin of individual strata has not yet been explained hydraulically; most probably, diverse mechanisms have operated. The dynamics of sedimentation of these facies can be interpreted better in terms of the depositional environment; this discussion is deferred to the section on associations of facies.

4.1.3 E Facies (Chaotic Facies)

Within this vast category we grouped for convenience all deposits that originated within rather than outside the sedimentary as a result of remobilization by either massive sliding or tangential slips, independent of the ultimate or immediate cause of the collapse and of the rheological behavior of the materials. Many aspects of this deposits can be studied such as their composition, the intensity and style of deformation, and then scale of deformation. The term chaotic is used here in a general sense, and includes mild and /or localized deformation of beds. Excluded, however, are chaotic intervals or levels within individual beds, which belong to other facies.

The strata are represented by a sandstone bed of extremely variable lateral thickness. Chaotic interval composed of a pelitic matrix that includes sandstone, within the sandstone of a part T_{b-e} sequence; the oblique laminae is of a variable thickness and locally discontinuous. In the study area, deposits formed by submarine sliding have been described, particularly in Oligocene formations.

5. CONCLUSION

The shales in the Western Marmara, Tekirdağ basin, contain a greater proportion of smectite, mixed-layer clay and less illite than do the associated turbidite sandstones. Size fractions demonstrate the greater concentration of smectite and mixed-layer clay in the very fine fractions whereas illite is at a maximum in the 2-4 µm size range. Separated < 2 µm fractions from the shales and sandstones show reduced illite contents compared with the whole rock, confirming the grain size control on the mineralogy, but the clay fractions from the shales and sandstones still remain significantly different. The shales in the study area have a higher ratio of smectite to illite plus mixed-layer clay than do the more basinal shales. A model based on progressive changes in clay proportions with distance from the shoreline is proposed in which the role of the turbidity currents has been to transport sediment into a deeper water environment without additional sorting. The shale clasts in the turbidite sandstones are approximately contemporaneous with sedimentation, based on the palynology. The clay mineralogy of the clasts is distinctive and differs considerably from that of the sandstone matrix. The depositional environment from which the clasts were eroded by the currents is, however, uncertain at this stage. The quartz content is a measure of the grain size and graded bedding occurs in the sandstone units. The shales do not show any systematic vertical variations in quartz content, indicating a non-turbiditic origin. In the field, a graduation from shale to fine-grained sandstone is visible, the analyzed samples reveal that any gradation must be over short vertical thicknesses and not through the shale units. The mineralogy of the samples provides information in support of the clay model outlined above. From a consideration of the A1203 vs Ti02, relationships, it is concluded that there is a compositional difference between the matrix in the sandstones and the shales, which is consistent with what is known of the clay assemblages. In contrast, the shale values cluster, which is indicative of a hemipelagic, turbiditic origin.

The sandstones are greywackes however, and open system conditions would not have prevailed for as long compared with more permeable sandstones. The shales and the sandstones in the Western Marmara region contain only minor amounts of precipitate/diagenetic minerals and organic carbon; the latter could well be dominantly of terrestrial origin. These components do not, therefore, have the same interpretative value in a relatively shallow water basin, dominated by a terrigenous input, as in present-day, deep-ocean environments.

Several factors caused considerable variation in the diagenetic history of the facies described, with subsequent strong influence on the characteristics of the sandstones as reflected in their porosity and permeability. In both the Eocene fluvial (facies D) and Oligocene paralic deposits (facies E/F), the environment of deposition strongly controlled the early diagenetic history. The early formation of clay minerals, particularly smectite and illite-smectite in the Eocene fluvial deposits, appears to have inhibited pressure solution of the framework grains later during burial diagenesis. In the Eocene sandstones smectite effectively destroyed permeability, but the illite in the Oligocene sandstones was less damaging to permeability.

In the two examples of marine turbidite deposits, alkaline porewaters of marine origin prevented the alteration of framework grains during early diagenesis since micas and feldspars are essentially stable under alkaline conditions (Velde, 1983; Bjørlykke, 1983). Later, during burial diagenesis, dissolution at grain contacts with subsequent reprecipitation controlled the formation of authigenic minerals.

The pH of the original pore-waters, itself a factor of climate, original depositional environment and rock composition, strongly controlled early diagenesis. Dissolution of the framework grains was influenced to a large extent by the presence or absence of earlier formed diagenetic clay minerals and detrital grains such as muscovite, carbonate shell fragments. Local variations in cementation can be linked with organic content and are probably due to solution effects due to carboxylic acid production during organic maturation. variation in quartz cementation was related to dewatering of adjacent shales, and produced an early generation of small, double-ended quartz crystals prior to quartz overgrowth formation. The original detrital mineralogy, organic content and depositional environment strongly influenced the later burial diagenesis of the sandstones. Within each facies described the coarser, better sorted, sandstones have the best reservoir characteristics, except where late diagenetic carbonate cementation has taken place.

REFERENCES

Adams, A. E., MacKenzie, W. S. and Guilford, C., 1988. Atlas of sedimentary rocks under the microscope. Great Britain, Longman Group UK Ltd.

Aigner, T. and Bachmann, G.-H., 1992. Sequence-stratigraphic framework of the German Triassic. Sedimentary Geology 80, 115-135.

Almon, W. R., 1981. Depositional environment and diagenesis of Permian Rotliegendes sandstones in the Dutch sector of the Southern North Sea. − In: Longstaffe, F.J. (ed.), Clays and the Resource Geologist, Mineral. Association Canada Short Course Handbook 7, 119-147.

Altermann, W., Drobek, T., Frei, M., Heckl, W. M., Kantioler, M., Lieu, K. P., Stark, R. W. and Strobel, C., 2010. Surface and Wetting Properties of Diagenetic Minerals and Sedimentary Grains in Reservoir Rocks (NanoPorO). Geotechnologien Science Report 16, 65-75.

Altermann, W., Stark, R. W., Drobek, T., Frei, M., Lieu, K. P. and Strobel, J. (2011). Nanomorphology and Wetting Properties of Sediment Grain and Porespace Surfaces (NanoPorO), Ludwig-Maximilians-UniversitätMünchen, Department für Geo- und Umweltwissenschaften.

Aral I. Okay, Okan Tüysüz, Şinasi Kaya, 2004. From transpression to transtension: changes in morphology and structure around a bend on the North Anatolian Fault in the Marmara region, 260-268.

Cai, J. C., Yu, B. M., Zou, M. Q. and Mei, M. F., 2010. Fractal Analysis of Surface Roughness of Particles in Porous Media. Chinese Physics Letters 27(2/024705), 1-4.

Chae, B. G., Ichikawa, Y., Jeong, G. C., Seo, Y. S. and Kim, B. C., 2004. Roughness measurement of rock discontinuities using a confocal laser scanning microscope and the Fourier spectral analysis. Engineering Geology 72, 181-199.

Choquette, P. W. and Pray, L. C., 1970. Geologic nomenclature and classification of porosity in sedimentary carbonates. Bulletin-American Association of Petroleum Geologists 54(2), 207-250.

Correns, C. W., 1950. ZurGeochemie der Diagenese. GeochimicaCosmochimicaActa 1, 49-54.

Dickinson, W. R., 1985. Interpreting detrital modes of greywack and arkose. Sedimentary Research 40(2), 695-707.

Diepenbroek, M., Bartholomä, A. and Ibbeken, H., 1992. How round is round? A new approach to the topic "roundness" by Fourier grain shape analysis. Sedimentology 39, 411-422.

Drobek, T., Kantioler, M., Lieu, K. P., Altermann, W., Frei, M., Strobel, J. and Stark, R. W., 2010. Pore surface topography in sandstone reservoirs. Schriftenreihe Deutsche GesellschaftGeowissenschaften (SDGG). 145-146.

Drolon, H., Druaux, F. and Faure, A., 2000. Particles shape analysis and classification using the wavelet transform. Pattern Recognition Letters 21, 473-482.

E. Mutti and F.RicciLucci, 1978. Turbidites of the Northern Appenines, 127-139

Gaupp, R., 1996. Diagenesis types and their application in diagenesis mapping. − Zbl. Geologie und Paläontologie 1, 1994(11/12), 1183-1199.

Gaupp, R., Gast, R. and Forster, C., 2000. Late Permian Playa Lake Deposits of the Southern Permian Basin (Central Europe). − In: Gierlowski-Kordesch, E.H. and Kelts, K.R. (eds.), Lake basins through space and time. AAPG Studies in Geology 46, 75-86.

Goes, S., Loohuis, J. J. P., Wortel, M. J. R. and Govers, R., 2000. The effect of plate stresses and shallow mantle temperatures on tectonics of northwestern Europe. Global and Planetary Change 27, 23-38.

Hayes, J. B., 1970. Polytypism of chlorite in sedimentary rocks. Clay Mineral 18, 285-306.

I.S.C. Spark and N.H. Trewin, 1985. Facies related diagenesis in the main claymore oilfiled sandstones, 479-496

McCann, T., 1996. Pre-Permian of the north-east German Basin. Geology 31, 159-177.

McCann, T., 1998. Sandstone composition and provenance of the Rotliegend of the NE German Basin. Sedimentary Geology 116, 177-198.

Menéndez, B., David, C. and Nistal, A. M., 2001. Confocal scanning laser microscope applied to the study of pore and crack networks in rocks. Computer and Geosciences 27, 1101-1109.

Pettijohn, F. J., 1975. Sedimentary rock, Harper & Row.

Pettijohn, F. J., Potter, P. E. and Siever, R., 1972. Sand and sandstone, Springer-VerlagBerlin.Heidelberg.

Seemann, U., 1982. Depositional facies, diagenetic clay minerals and reservoir quality of Rotliegend sediments in the Southern Permian Basin (North Sea). Clay Mineral 17, 55-67.

Wilson, M. D., 1992. Inherited grain-rimming clays in sandstones from eolian and shelf environments: Their origin and control on reservoir properties. - In: Houseknecht, D.W and Pittman, E.D. (eds.), Origin, Diagenesis, and Petrophysiscs of Clay Minerals in Sandstones SEPM Special Publications 47, 209-225; Tulsa.

APPENDICES

APPENDIX A: Diagrams for estimation of grain sorting

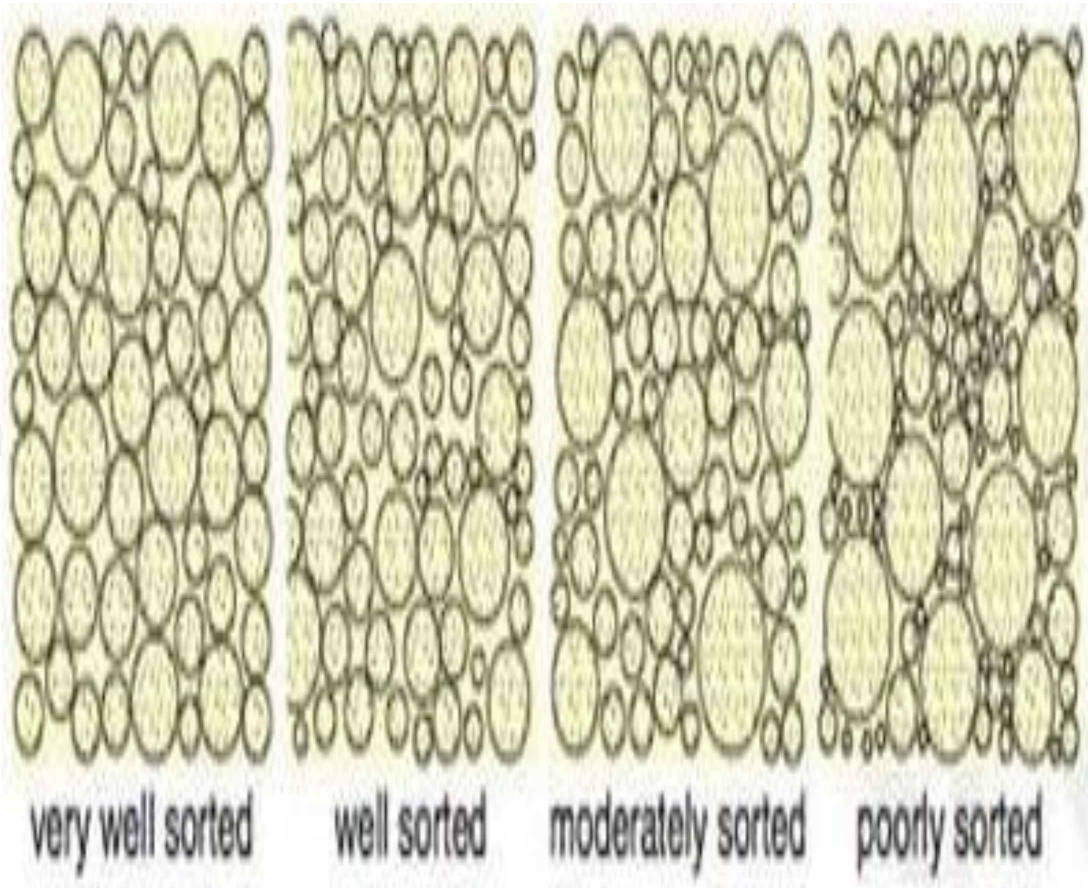

Figure A1: Sorting diagrams using thin sections (after Pettijohn et al. 1973)

APPENDIX B: Categories of roundness for grains

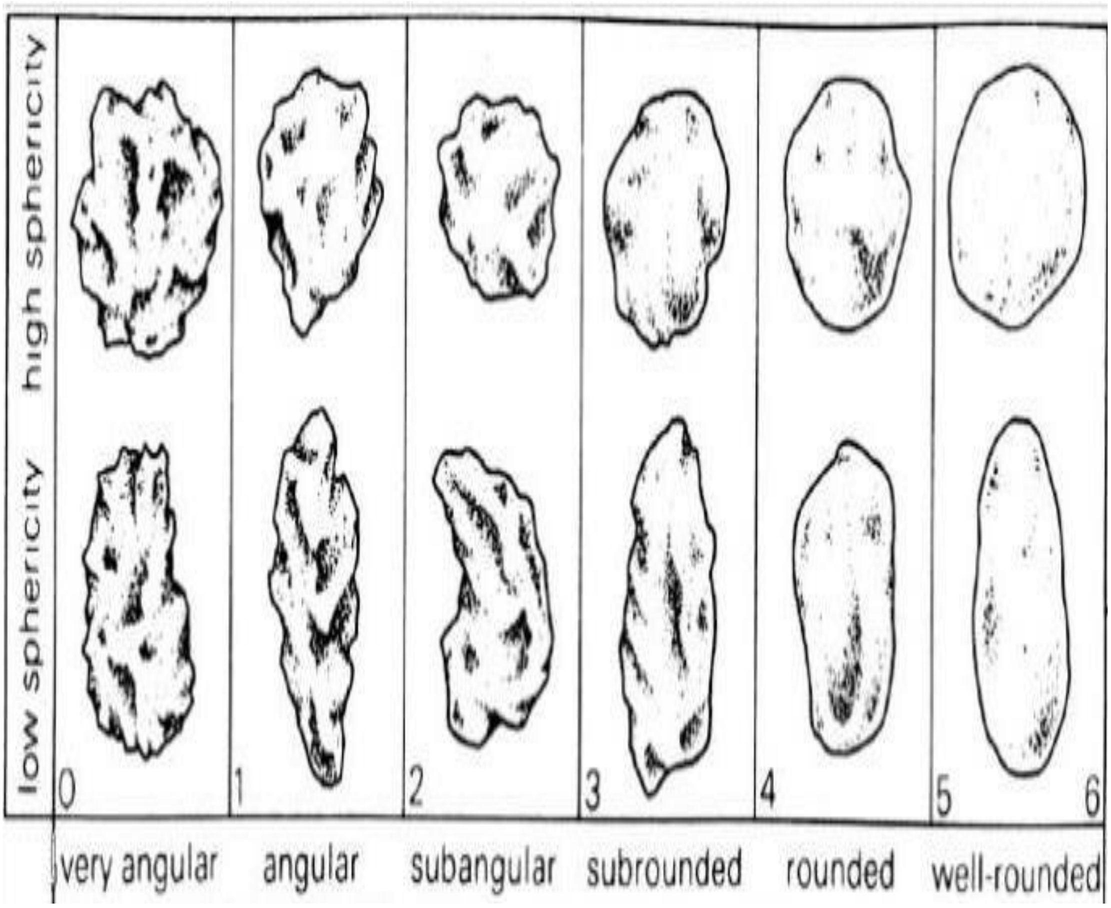

Figure A2: Categories of roundness for grain of low and high sphericity (after Pettijohn et al. 1973)

APPENDIX C: Grain Size Classification

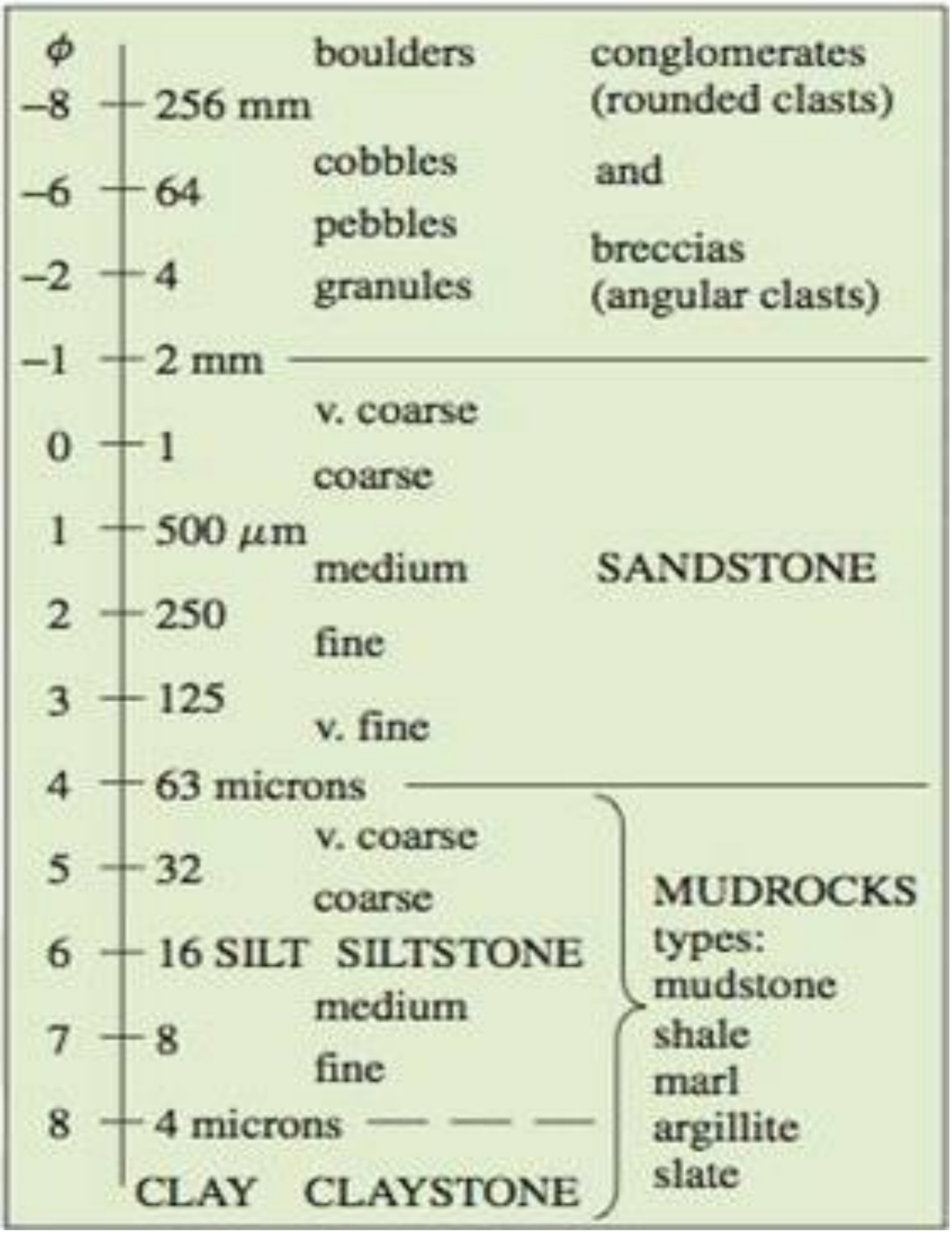

Figure A3: Grain size classification of sediments (Udden - Wentworth scale)

CURRICULUM VITAE (CV)

Full name: Havva GURZALIYEVA

Birth date and Place: 05.04.1990/ Baku, Azerbaijan

Address: st. F. Malikov 2A app.6, Baku, Azerbaijan

E-mail: gurzaliyeva_eva@live.ru

Education:

Bachelor’s degree: Azerbaijan State Oil Academy, **major:** Petroleum Engineer, 2008-2012

Work experience: **Wireline Engineer** - Schlumberger (Caspian Sea) Ltd., Baku, Azerbaijan; 01June-31August 2014;